Politecnico di Milano

SCHOOL OF INDUSTRIAL AND INFORMATION ENGINEERING
Master of Science – Energy Engineering

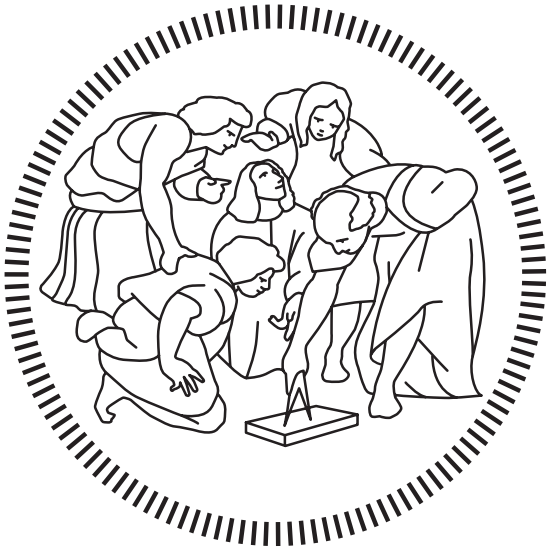

Design and Operation Optimisation of Highly Integrated CSP-PV Hybrid Power Plants

Supervisor
Title Name SURNAME

Co-Supervisor
Title Name SURNAME

Candidate
Marco Colombari – 914176

Academic Year 20XX – 20XX

Acknowledgements

Lorem ipsum dolor sit amet, consectetur adipisci elit, sed eiusmod tempor incidunt ut labore et dolore magna aliqua. Ut enim ad minim veniam, quis nostrum exercitationem ullam corporis suscipit laboriosam, nisi ut aliquid ex ea commodi consequatur. Quis aute iure reprehenderit in voluptate velit esse cillum dolore eu fugiat nulla pariatur. Excepteur sint obcaecat cupiditat non proident, sunt in culpa qui officia deserunt mollit anim id est laborum. Lorem ipsum dolor sit amet, consectetur adipisci elit, sed eiusmod tempor incidunt ut labore et dolore magna aliqua. Ut enim ad minim veniam, quis nostrum exercitationem ullam corporis suscipit laboriosam, nisi ut aliquid ex ea commodi consequatur. Quis aute iure reprehenderit in voluptate velit esse cillum dolore eu fugiat nulla pariatur. Excepteur sint obcaecat cupiditat non proident, sunt in culpa qui officia deserunt mollit anim id est laborum. Lorem ipsum dolor sit amet, consectetur adipisci elit, sed eiusmod tempor incidunt ut labore et dolore magna aliqua. Ut enim ad minim veniam, quis nostrum exercitationem ullam corporis suscipit laboriosam, nisi ut aliquid ex ea commodi consequatur. Quis aute iure reprehenderit in voluptate velit esse cillum dolore eu fugiat nulla pariatur. Excepteur sint obcaecat cupiditat non proident, sunt in culpa qui officia deserunt mollit anim id est laborum.

Contents

Abstract

1 pag

Extended Abstract

4-5 pag

List of Figures

List of Tables

Introduction

Energy supply is among world's most current, influential and most fundamental problems these times. It concerns environmental, economical, technical, as well as social matters, and its root cause lies not only in the increase of the world population, but also in the fallacious and dazzling belief of unconstrained growth and power, in which part of that population has lived during the last centuries.

Most recently, however, the climate change seems to be a widely accepted fact and the public opinion is starting to push for a change, aiming for a sustainable way of living. In this regard, one of the indicators used to generally assess how well or bad the efforts made are performing is the CO_2-e concentration ("-e" stands for equivalent, i.e. equivalence is made in terms of Global Warming Potential, so that all the greenhouse gases emissions can be merged into a single voice), but most often the CO_2 alone is measured for simplicity. Measured data from 1750 to 2019 are shown in Figure 1. The figure only shows atmospheric CO_2 concentration data

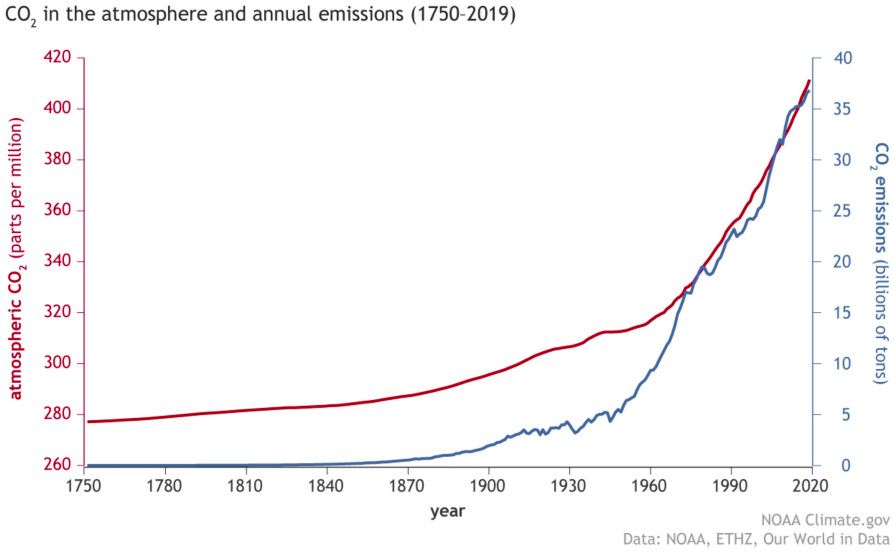

Figure 1. Atmospheric CO_2 concentration vs CO_2 emissions [1]

from mid-18th century, nevertheless carbon dioxide levels today are reported to be higher than at any point in at least the past 800,000 years [1]. In particular, a steep rise can be noticed starting from the 1950s, in correspondence with the intensification of anthropogenic activities. Such a high concentration of CO_2 and other greenhouse gases (GHGs) is related to average annual temperature, ocean acidification and other phenomena, the effects of which are outside the scope of this work.

How much of GHG emissions is associated to the electricity and heat production has been estimated at 30% of the total in 2016, the whole energy sector accounting for roughly 73% and the rest being mostly due to agriculture, forestry and land use (18% ca.) [2].

It is hence evident that a significant transformation of the global energy system is required. In this context, efforts have been made during the Paris Agreement signed in 2016, which is nowadays ratified by the vast majority of countries in the world and aims to limit the global warming. According to the International Energy Agency, in those years (2013-2016) the energy-related carbon dioxide emissions have been constant for a while, then increased in 2017 and 2018, and eventually they have been reported to be constant in 2019, flattening at around 33 gigatonnes (Gt). This last trend resulted mainly from a decline in CO_2 emissions from the power sector in advanced economies, thanks to the expanding role of Renewable Energy Sources (RES) systems (mainly wind turbines and solar PV), fuel switching from coal to natural gas, and higher nuclear power output [3]. Still according to IEA [4], the above-mentioned technologies will have the burden of meeting the expected growing energy demand of the next years. As a consequence of that and of the Paris agreement ratification, many states have developed policies to decrease their carbon footprint. Among those countries, the European Union with the European Green Deal has committed to achieve zero net GHG emissions by 2050. Figure 2 once again highlights the key role of renewables in the next future, in this case specific to the European context.

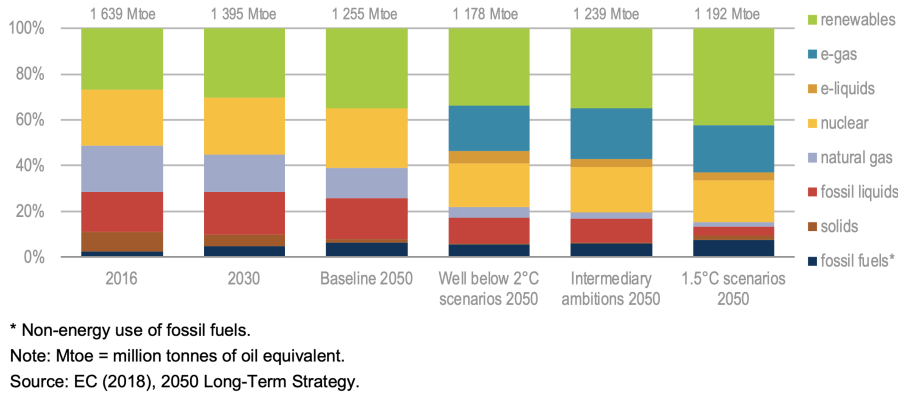

Figure 2. EU energy mix from 2016 to 2050 Long-Term Strategy scenarios [5]

Shifting the focus to the Italian energy sector, the National Energy Strategy 2017 [6], which lays down the actions to be achieved by 2030 in accordance with the EU Energy Roadmap 2050 and the future targets set by COP21, aims at a 28% share of renewables in total energy consumption, and at a 55% share in electricity consumption. Moreover, it includes the phase out of coal as a fuel in the electricity generation sector by 2025. The plan highlights that RES as wind and solar are the technologies with the highest residual potential still to be tapped, but also that this entails increasing the capacity of storage systems and implementing grid projects to guarantee energy security. The concept of "energy security" opens the way to the broader matter of "energy trilemma", which substantially states that it is nearly impossible to achieve energy security, energy equity, and environmental

sustainability at the same time, as described in Figure 3. Given the intrinsic

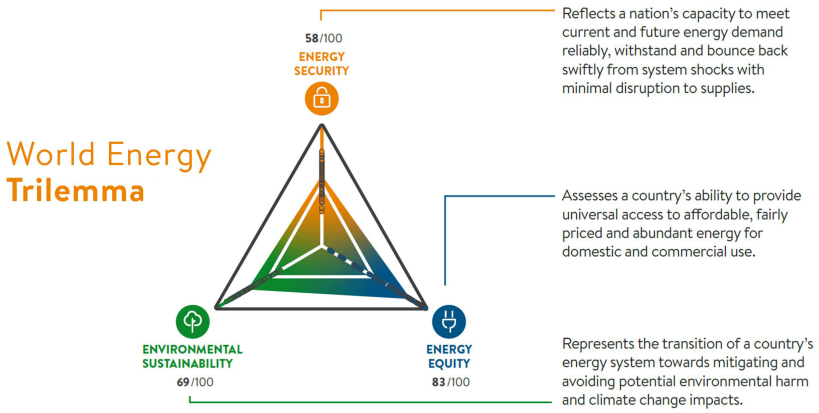

Figure 3. "Energy Trilemma" [7]

imposition of the Trilemma, the best achievable objective is to reach and keep a condition of good balance between the three "parties", other than scoring sufficient levels in each individual parameter.

Given the current situation, maintaining the balance in a context of rapid transition to decentralised, decarbonised and digital systems is a even more challenging task [7]. Indeed, the plummeting of PV modules cost in the last decades, which also led to the achievement of "grid parity" for this technology in a conspicuous number of markets [8, 9], could at first sight suggest that the Trilemma has been solved. However, low costs and reduced lifecycle Greenhouse Gas (GHG) emissions are not enough; As a matter of fact, these characteristics could even cause a strong unbalance of the "triangle" towards equity and sustainability, seriously jeopardising the energy security because of the peaks and valleys of the solar resource.

All of this leads to the need of including another key parameter in the analysis: dispatchability (i.e. capability of being dispatched on demand at the request of power grid operators, according to market needs), something that most of RES technologies as PV, wind, CSP can not guarantee without aids. That is where energy storage systems come into play. As can be imagined, such devices are becoming increasingly fundamental and inevitable, in parallel with the rapid deployment of wind and solar power generation. Energy storage systems can be installed integrated with the RES production plants, increasing their dispatchability up to what is typical of coal or even gas combined cycle power plants; Alternatively, storage units can be installed along the grid to "bring relief" in areas subject to strong peaks and valleys, that would otherwise require either curtailment of some production units, or costly oversizing of the transmission network. As Ref. [10] details, these kinds of “storage facilities” can offer "ancillary services" (short response time and limited storage reserve capacity applications), or "bulk energy services" (storage of large amounts of energy, such as time-shifting[1] and load following), depending on

[1]Electric energy time-shifting involves purchasing inexpensive electric energy, available during periods when prices or system marginal costs are low, to charge the storage system so that the

their characteristics.

Considering again the recent PV phenomenon mentioned above, from an exergy point of view, the most appropriate commercial storage technology to be coupled with PV is the battery. In particular, lithium batteries have been proven feasible for industrialization and well performing compared to other kinds of available batteries. However, at the time of writing, in applications where energy density is not a key parameter, as in stationary power reserves, lithium is often not the most economically favourable option, in addition to being ethically and environmentally questionable due to the extraction processes of some components of the batteries based on this material.

PV is not the only technology competing for the solar resource, as it can be expected looking as an example at the study conducted by JRC EU [11], in which it has been estimated that the solar potential of the European Union would be sufficient to cover three times its 2016 electricity demand, requiring as little as 1-2% of EU's land. On the other side of the ring, CSP "more traditionally" relies on heat as a means for eventually producing electricity. CSP alone is not nearly as cheap as PV, even though its costs have seen a strong reduction, too [12]; moreover, it is not feasible for residential-scale purposes. Nevertheless, it can be coupled quite easily and with modest exergy destruction with low-cost Thermal Energy Storage (TES), allowing for an increased dispatchability and making it competitive with PV in certain areas.

As a consequence of the characteristic drawbacks of both sides described above, in the last years the concept of hybridization (i.e. combining together different technologies to obtain more efficient and/or cheaper solutions) is emerging in the RES field. In fact, on the one hand PV is cheap but not dispatchable, on the other hand CSP+TES is more expensive but more dispatchable. Moreover, CSP+TES exploits Power Block (PB) technologies long developed for conventional generation plants, often characterised by bigger sizes and lower flexibility than what CSP would require, resulting in techno-economic performance downrating compared to "traditional" applications.

Starke et al. [13] compared different possible CSP-PV plants in Chile with stand alone CSP's using the same technologies in a multi-objective optimisation context, obtaining both higher Capacity Factor (CF) and lower Levelised Cost Of Electricity (LCOE) for the hybrid solution. Same results have been obtained in Ref. [14]. A comparison with PV-BESS power plants is instead more difficult for several reasons: to the author's knowledge, there are no utility-scale power plants of this kind; PV and Lithium battery storage costs have been strongly decreasing recently; Geographical location and financial and operating strategy assumptions significantly influence the results as well. Ref.'s [15], [16] and [17] return indeed rather variable results for the same analysed technology. Nevertheless, a 2016 study by NREL highlighted how the PV-BESS should not be competitive with CSP even in 2030 for storage sizes greater than 2-3 hours [18].

At the time of writing there exist few practical examples of CSP-PV, but some more are under construction in favourable areas as the Redstone power plant in

stored energy can be used or sold at a later time when the price or costs are high (i.e. operate price arbitrage).

South Africa, and the record-breaking 950MW Noor Energy 1 in Dubai. The 110MW CSP, 100MW PV Cerro Dominador plant in Chile is the only operating commercial example of CSP-PV hybrid plant [19]. However, the hybridization in this case only consists in figuring as a single power plant from the point of view of the grid. The PV and CSP sections are indeed operated together in order to meet the required objectives, but by no means can physically interact with one another. Petrollese et al., University of Cagliari [20], developed a pilot CSP-CPV power plant installed in Ottana, Sardinia, with respectively 630 kW and 400 kW nominal powers of the two subsections. The Ottana facility also includes a 430 kWh Sodium-Nickel battery bank coupled with the Concentrated Photovoltaic (CPV) subsystem intended for short-term energy storage. However, besides this additional component, the integration level is the same as for the Cerro Dominador plant. The approved 800MW Noor Midelt in Morocco scheduled to start operation in 2022 is the only one with a higher level of integration, including not only a thermal and a battery storage, but also an "eTES" system so that PV is capable of charging the thermal storage when needed [21]. In this context, the main purpose of this thesis regards the optimisation of the design and operation of different possible power plants to be located in Italy, based on highly integrated CSP-PV technology and providing a good level of dispatchability, according to possible requirements of the investor. The analysis is well suited to a background in which Sicily is foreseen as an important hub for green hydrogen in the near future. Indeed, according to a report by SNAM and McKinsey, green hydrogen will become the cheapest source of hydrogen by 2030, with Italy anticipating other European markets thanks to solar resource availability [22]. Also, it has been argued that Sicily may become an intermediate stop-over for hydrogen produced in North Africa, utilizing the transport infrastructure connecting North Africa and Italy [22, 23].

Work Outline

The purpose of this work is to develop a tool able to optimise the design and operation of various possible hybrid CSP-PV power plant configurations, which can operate following different electricity demand profiles and in different market/incentive contexts. This kind of plants can help to safely achieve higher levels of RES penetration in the power grid, thanks to the higher dispatchability that can be obtained.

After the introduction of the state of the art of the technology in solar power plants, outlining the basic principles of operation and the relevant subsystems, a review of the hybridisation possibilities of such plants is presented.

Chapter 2 presents a summary of the optimisation techniques adopted in relevant literature about the topic, highlighting their main pros and cons. Approaches to deal with input uncertainties are introduced as well.

In chapter 3 possible supercritical CO2 cycle configurations are proposed, since, for an indirect plant configuration, the working fluid and the HTF are different; the choice of CO2 closed cycles instead of conventional Rankine cy- cles presents substantial advantages, in terms of compactness, fast response to transient conditions and better thermodynamic efficiency. Chapter 4 explains in deta

Chapter 1

Technologies in Solar Power Plants

The first chapter of this dissertation gives an overview of the technologies used in solar power plants, introducing the state of the art, the characteristics and functionalities of the main subsystems and components used in applications aimed to the production of electrical energy.

1.1 Concentrated Solar Power Systems

CSP technologies exploit the direct solar radiation in order to generate useful heat to be processed typically by a turbine, the work of which can be eventually converted into electrical energy. The incoming Direct Normal Irradiance (DNI) is redirected onto a receiver by means of reflecting mirrors (concentrators), in this way a large area of solar radiation can be focused on a small area (receiver) containing a flowing Heat Transfer Fluid (HTF), which temperature is thereby increased. The thermal energy content of the HTF is then exploited by a thermodynamic power cycle, which produces mechanical work easily convertible into electrical energy through an alternator. CSP plants are often also equipped with a TES. The storage of thermal energy is indeed relatively cheap and allows to achieve higher dispatchability, being the plant able to draw on the reserve during night or periods of bad weather. As outlined in the Introduction, compared to most RES, such plants are characterised by higher dispatchability but also by higher costs due to still not large deployment and adaptation of "traditional" technology not designed for flexibility.

There exist different configurations and technologies of CSP, however, the subsystems that characterise them are the following:

- Solar energy collection system, composed by:
  - Concentrators (mirrors)
  - Receiver(s)
- Power Block, the main components of which are:
  - Heating line heat exchangers
  - Turbomachinery

  - Heat rejection system

- Thermal Energy Storage (when present)

Solar energy collection systems can be classified as shown in Figure 1.1.

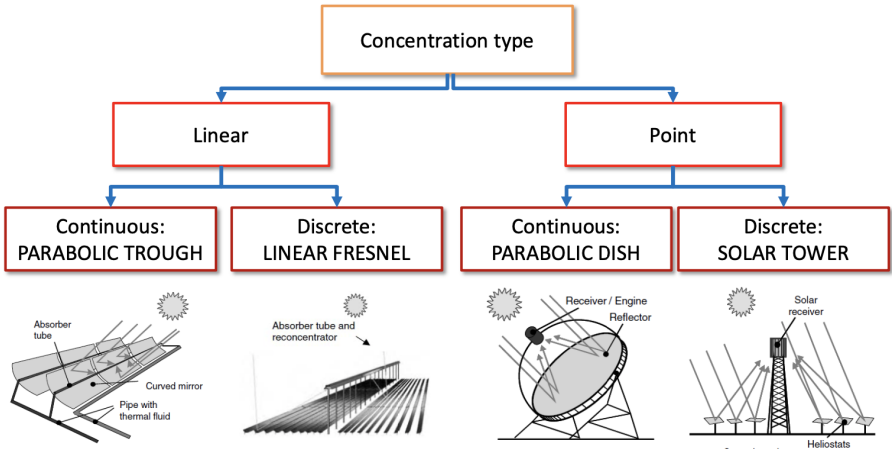

Figure 1.1. CSP solar energy collection technologies

Linear focus systems are characterised by lower Concentration Ratio (CR) (i.e. the ratio between the receiver area and the solar field (mirrors) area) compared to point-focus ones, which results in lower thermal efficiency under the same temperatures. Moreover, the sun tracking of linear collectors is constrained to 1 axis, resulting in lower average yearly optical efficiency. However, despite these disadvantages, linear technologies can still be the best choice depending on the context, because of the following reasons:

- Parabolic dishes score the highest solar to electric efficiency, but they can not be easily coupled with TES, they are limited in size so that there are no scale-up benefits, and the Stirling cycles used have not given proof of good reliability so far. All these elements combined with the falling price of PV have strongly limited the practical implementation of this technology.
- Solar towers are typically characterised by great overall performances. However, this kind of systems typically implies more sophisticated technologies especially in the receiver; the tower and receiver have a significant economic scale effect favouring bigger plant sizes; the height of the tower (ground heights can even reach 250m) causes a more noticeable environmental impact; the greater complexity and investment costs reduce the "bankability" of solar towers compared to the most historically established Parabolic Trough (PT) technology.

Focusing on the differences between the two linear technologies represented in Figure 1.1, it can be noticed that the Linear Fresnel (LF) is composed by rows of near-ground level mirrors mimicking the shape of the PT parabola. For this reason and because of the higher CR of the LF, the optical efficiency (i.e.

the ratio between the radiation on the receiver and the DNI on the mirror) is lower than in the PT case. However, LF mirrors are easier to produce and cheaper, they need less robust mounting owing to lower wind impact, and the land use factor (hereby referred to as Ground Coverage Ratio (GCR)[1]) can achieve higher values since no significant self shading occurs between rows.

GCR has the highest values in the LF case, followed by PT. Solar towers instead require vast areas of land due to 2-axis tracing heliostats and to the need to limit the self-shadowing and blocking (i.e. sun rays reflected hitting the back of another mirror) losses.

Each of the above-mentioned optical technologies has a HTF flowing in the receiver(s), the choice of which is also connected to the optical technology chosen.

PT's are usually equipped with thermal oil: on the one hand synthetic oil has a low maximum operating temperature (about 390°C) due to thermal instability phenomena, limiting the PB efficiency, on the other hand a lower maximum temperature reduces thermal losses. Also, thermal oils are characterised by solidification temperatures of about 10-20°C, so that possible freezing during cold periods without solar radiation is often not a very complex issue. Current research is evaluating the possibility of using molten salts in PT's [24], these compounds are characterised by higher operating temperatures (e.g. the most used one, "solar salt": 240-565°C ca.), causing serious anti-freezing countermeasures to be taken and relevant thermal losses from the long receiver piping during night and bad weather periods. Moreover, technical challenges arise because the receiver tubes in which the HTF flows move together with the troughs, requiring flexible hoses that must withstand fatigue stress under high temperature conditions to avoid leaks [25].

LF's, unlike PT's, have a fixed receiver, thus eliminating the issues related to its movement. It follows that this technology has been mainly developed with Direct Steam Generation (DSG) or molten salts [26]. DSG has the advantage of being also the power cycle working fluid in the case of steam ranking cycles, but thermal storage in this case is not straightforward (unless a different substance is used for storing energy, installing Heat Exchanger (HX)'s and partially losing the advantages of this technology) and the management is complicated in transients due to the phase change of water, even more if higher temperatures are to be achieved and superheated steam is involved. As described above, if molten salts are used as HTF, it is possible to obtain a high PB nominal efficiency in the case of steam Rankine cycles, but anti-freezing techniques must be adopted and thermal losses during non-production periods must be considered similarly to the PT case.

In solar towers, compared to linear technologies, the HTF is not exposed to the environment in long tubes, with the consequence of strongly reduced fluid freezing-related issues. In this case the common HTF choice among the commercially available solutions is the use of molten salts, since it allows higher PB performances and is cheaper than thermal oil, too. Research is

[1] GCR: active area to used land ratio.

investigating the use of liquid sodium in particular for tower applications, indeed, not only thanks to its larger operating temperature range it would increase the PB performances, but also owing to its high thermal conductivity it would increase significantly the admissible heat flux on the receiver. However, there is skepticism on sodium as HTF due to flammability and corrosion issues which caused CSP accidents in the past [27].

Power Blocks The choice of the PB is mainly related to the size of the plant, but it is also linked to the HTF choice, being the operating temperatures different from fluid to fluid. Commercially used power cycles for CSP applications are Organic Rankine Cycle (ORC) and Steam Rankine Cycle (SRC).

ORC's are the best choice for small plants ($\lesssim$ 5 MW), since they offer a simpler design and more flexibility than SRC's; as a drawback, their operating temperature is limited to about 400°C due to thermal stability issues of the working fluids, making these PB's optimal for small size solar fields using oil as HTF.

SRC's can instead work with higher temperatures, optimal to be coupled with molten salts solar fields, achieving higher nominal efficiencies than ORC's; they are better-suited for sizes ($\gtrsim$ 10 MW) because of expander design difficulties linked to the low steam flow rates.

In order to be able to exploit high temperature heat that could possibly be provided by HTF's such as liquid sodium, a lot of effort has been put in the research for a power cycle that would best the performances of SRC's, which has limits such as a maximum Turbine Inlet Temperature (TIT) of about 600°C due to corrosion effects, considerable thermal inertia in the subcritical case, design complications for power sizes typical of CSP plants in the supercritical case. A promising solution seems to be the Supercritical CO_2 (sCO_2) cycle, which combines characteristics of both gas and Rankine cycles: possibility of achieving high TIT with less material issues; much smaller components and lower inertia compared to SRC's thanks to CO_2 properties; limited compression work, since the fluid enters the compressor near the critical point. However, warm/hot climates could significantly affect the efficiency in case of air-cooling, more complex layouts as recompressed cycles should be used, turbomachinery efficiency must be very high and large-scale plants are still to be proved.

Thermal Energy Storage Systems : A first distinction among the heat storage system is whether the storage is "direct" or "indirect", i.e. the substance in the storage is the same as the HTF so that a direct connection is possible, or the HTF and the storage content and different, so that a HX is needed (with relative costs and heat transfer losses). For example, a drawback of oil-based solar energy collection systems is that they must rely on indirect TES, due to the relatively high price of thermal oil.

The "classical" configuration requires two tanks (more if modular tanks are used): one "hot tank" and one "cold tank". However, this configuration requires to double the tank capacity compared to what would theoretically

be necessary. A solution may lie in the "thermocline" technology, but as drawbacks, at the state of the art, the temperatures in the vessel would be lower than T_{max} and higher than T_{min} affecting the thermal to power conversion efficiency and amount of energy stored, connected to the heat degradation with time as consequence of the diffusion.

A further distinction can be made based on whether latent heat or sensible heat is stored: the last one is the case for example of molten salts, stored in their liquid phase, while the first one relies on Phase Change Material (PCM)'s, generally allowing higher energy densities, as it is the case 1414's silicon-based system currently under testing [28]. Packed-bed solid sensible heat storage systems are being investigating as well, in the perspective of enabling operation at higher temperatures and eventually achieving higher solar-to-electric efficiencies [29].

Thermo-chemical storage is another possible option but it is still not sufficiently investigated [29].

That being said, the widely commercially used solution is the 2-tank system with molten salts, thanks to the properties, to the relatively low cost, and to the experience that firms have acquired with this kind of compounds, other than to the simplicity of such a system compared to others.

As can be imagined from what above, there is neither a single solution nor some "silver bullet" solutions in the CSP field, but rather a wide variety of possible combinations, the optimum depending on the location, objectives, and project constraints, thus giving rise to a not trivial engineering problem.

1.2 Utility-scale Photovoltaics

Photovoltaic-based solar conversion technologies are usually inherently more straightforward than Concentrated Solar Power. The photovoltaic effect indeed enables a direct generation of electrical energy from the sunlight hitting a PV module.

The single generating elements, called "cells", are connected in series in a number most often varying between 60, 72 or 96, thus forming a "module". Generally, more than one module (i.e. an assembly of photovoltaic cells mounted in a framework for installation, often colloquially referred to as a panel) is connected in series, forming a "string". Strings can be eventually connected in parallel to form a PV "array".

For the same power output, there may be more shorter strings (i.e. lower voltage strings), or less longer strings (i.e. higher voltage strings) connected in parallel. On the one hand high voltage strings would minimise DC wiring losses and would require smaller cables, on the other hand this kind of solution is more subject to array mismatch losses (i.e. the difference between the sum of the powers of the modules taken alone and the array power) [30]. Also, the choice of the string voltage and the number of strings is related to the inverter choice. Indeed, the inverter not only converts the DC output coming from the modules into grid-friendly AC power, but also sets limits to the voltage range and to the maximum current to be processed, and operates the PV array (or string(s)) voltages in order to maximise the power output via the so called Maximum Power Point Tracking (MPPT).

The two main inverter options available for utility-scale PV systems are:

- string inverters
- central inverters

String inverters are connected to the electric terminals of each string, hence the MPPT is quite accurate thanks to the limited number of modules connected (which might be subject to different irradiation, temperature, soiling, faults).

Central inverters are bigger than string inverters, so that they can handle entire arrays, or sub-arrays in case they are equipped with multiple MPPT's. In this case, having a large number of modules connected, even with multiple MPPT's, the MPPT is intrinsically less detailed, resulting in increased mismatch losses. Moreover, central inverters require longer DC wiring, which implies greater losses or greater wiring expenses; also, the redundancy of these systems is lower and the maintenance may require highly qualified technicians. However, the specific CAPEX of central inverters is significantly lower and their efficiency tends to be slightly higher compared to string inverters [31].

That said, utility-scale photovoltaics are usually located in well-insolated plain areas, resulting in a rather uniform solar irradiance over the PV field (except for the effect of possible clouds). In such conditions, the magnitude of mismatch losses is reduced, so that central inverter, being cheaper is largely the most used type in large scale PV power plants [32].

There exist several types of PV technologies, some of which widely diffused and many others still under research or in pre-commercial phase.

Nowadays, the cell materials more suitable for utility-scale PV plants are the mono-crystalline silicon and multi-crystalline silicon. The first is characterised by higher efficiency (19%-20% nominal) and typically higher costs, while the second one by lower efficiency (16%-17% nominal) and typically lower costs. However, as PV systems are rapidly spreading, so are the industry trends, resulting in a recent marked drop of mono-crystalline silicon modules price thus increasing their competitiveness. In these regards, the technology roadmap is far from clear and stable, making the designer choice not obvious [33].

Among the cell materials still not commercially diffused, the most promising one seems to be the Perovskite, which has great efficiency, especially in tandem architecture with silicon, and a significantly lower cost. The drawbacks that are preventing this technology from a wide market reach are: rapid degradation (at the moment these cells preserve their characteristics for about 1 year); replicability (same performances must be obtained for all the produced cells and modules in order to overcome the early-commercial phase) [34].

A PV technology worth mentioning is the CPV, which as its name suggests concentrates sunlight onto the active surface area of the module, and it is currently the solar technology with the highest conversion efficiency (about 46%) owing to the use of high concentrating optics and multi-junction solar cells [35]. An analysis conducted by the Fraunhofer Institute for Solar Energy Systems indicated that in 2013 the CPV had a higher LCOE than PV, but with an increasing competitiveness by 2030 [36], so that it could become a valid solution in case of restricted land

area availability. In these regards, a 1 MW CPV-CSP pilot power plant based in Ottana, Sardinia has been in operation since September 2017 [20].

Also, "bifacial" or "double-sided" photovoltaic panels seem to be approaching the market. These panels, based on Hetero Junction Technology (HJT) cells which combine amorphous and crystalline silicon, can collect light from the front, and scattered and diffuse light falling on the backside of the cell itself. Looking at the Italian context, a "sun factory" located in Sicily has become an international centre of excellence in the photovoltaic industry, and in particular in the production of such PV technology.

To close the analysis of utility-scale PV systems, it must be highlighted that there exist different mounting/tracking possibilities.

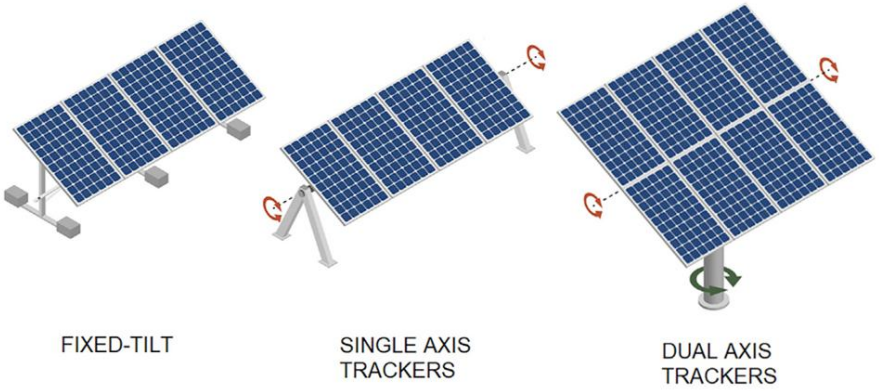

Figure 1.2. PV fixed mounting and tracking types [37]

The easiest and classic is the fixed-type mounting, so that PV modules are arranged in long parallel rows (each composed of 1 or 2 modules in parallel) with fixed azimuth (typically 0° or 180° depending on the hemisphere) and fixed tilt. In this case the tilt angle is usually optimised in order to maximise the yearly energy yield, according to geographical coordinates, surroundings possibly casting shadows on the strings, typical weather of the selected location.

The next step is the single-axis tracker. In this configuration rows of PV modules are aligned in parallel in north-south direction, the tracker follows the sun position from east to west. The axis of the tracker is usually horizontal, but it can also be tilted (TSAT). Single-axis tracking is gaining more and more attention in utility-scale PV farms, enough to account for approximately the 50% of the U.S. operating capacity of PV plants sized 1 MW or more [38]. This solution increases the plant investment costs, but generally increases the yearly energy yield as well.

Lastly, the dual-axis tracking system. This configuration sees rectangular-shaped groups of panels mounted on a structure equipped with two rotating axes, one vertical and one horizontal, so that theoretically the incidence angle (i.e. the angle between the normal to the PV module surface and the vector of the incoming sun radiation) is always 0°. In this case the energy yield is the highest, but so are investment costs, because of the limited number of modules per tracking assembly and increased complexity.

Comparing the three presented mounting/tracking systems, a recent study by C. D. Rodríguez-Gallegos et al. from several universities and institutions [37] has found that single-axis trackers with bifacial modules achieve the lowest LCOE (16% reduction on average with respect to conventional mono-facial fixed-tilt) in the majority of world locations (93.1% of the land area), and the yield is boosted by 35%; their mono-facial counterparts achieve the lowest LCOE in only 3.1%. Instead, even though bifacial dual-axis trackers increase the yield by 40%, reach the lowest LCOE only for remote areas very close to the poles, at latitudes beyond 70°, accounting for 3.8% of the total land area. The reason behind that, as explained above, lies in the fact that while one-axis tracker installations typically incur less than 10% higher system costs, two-axis tracker installations are between 30% and 60% more expensive than conventional mono-facial fixed-tilt installations. With regard to fixed-tilt installations, bifacial fixed-tilt installations feature higher LCOE values close to the equator compared to mono-facial.

1.3 Battery Energy Storage Systems

Batteries are electrochemical energy storage devices, typically they receive electricity as input, store it in the form of chemical bonds, and eventually return the most of it as electric energy.

In an electric power plant, compared to TES they are generally characterised by faster response times, also because their output just needs to be processed by a power electronic device in case AC is needed. Another important point that must be stressed is the high cost of such devices, which so far has partially limited their commercial application. However, backed by Battery Electric Vehicle (BEV) deployment and many other market demands pushing the industry and the research, in the last years Battery Energy Storage System (BESS)'s have experienced a cost reduction which is expected to increase the profitability of batteries to be deployed in utility-scale electricity generation systems [39].

Currently, for what concerns stationary storage grid applications, the most used BESS technologies are lithium-ion and lead acid. Lead acid is the "traditional" technology in the battery field, it has lower upfront cost compared to lithium batteries, but lower Depth of Discharge (DoD)[2], less life cycles, other than a round-trip DC-to-DC efficiency[3] of 76–82% compared to 94–98%. According to IRENA:

> Different battery storage technologies, such as lithium-ion (Li-ion), sodium sulphur and lead acid batteries, can be used for grid applications. However, in recent years, most of the market growth has been seen in Li-ion batteries. [40]

This is reflected in what found in the recent literature works about PV-CSP in which batteries were used, where Moser et al. [41], Zurita et al. [42], Hamilton

[2]DoD: it indicates the percentage of the battery discharged relative to the overall capacity of the battery.

[3]round-trip efficiency: the ratio between discharged energy and charged energy, i.e. the fraction of energy put into the storage that can be retrieved.

et al. [43] have used Li-ion, Zurita et al. [44] has used lead acid, and the above-mentioned pilot plant in Ottana uses a battery bank based on Sodium–Nickel which has no electrochemical self-discharge thanks to the ceramic electrolyte [45].

Another possibility suitable for stationary applications is the Vanadium Redox Flow Battery (VRFB) technology, the costs of which are decreasing as well and has the main advantages of a long lifetime and of decoupling energy capacity and maximum power output thanks to its electrolyte tanks and stack configuration, being instead penalised by lower power and energy density and round-trip efficiency. However, for this reason, the economic performance of VRFB's is improved for longer storage times than for Li-ion batteries, getting them to compete against other more mature storage technologies.

Going back to the most diffused Li-ion, as pointed out in the Introduction, environmental and ethical concerns are being raised because of some rare materials needed for this kind of battery. So, possibly owing to these concerns and to the above-explained economic reasons, other than to market logic, so far stationary utility-scale batteries are mainly used for power quality regulation and/or short term energy storage. Accordingly, in the work regarding the Ottana pilot power plant presented by Cau et al. [46], Sodium–Nickel batteries were introduced for the short-term energy storage and to smooth the fluctuation in the CPV power production. Therefore, they had a low storage capacity (about 1 h) unlike the TES system, which is more suitable for a medium-term energy storage. In addition to that, the batteries were used to fill the gap between the real and the expected power production, compensating for forecasting errors. Zhai et al. [47] optimized a hybrid CSP-PV plant to achieve the lowest LCOE, obtaining better results with a small battery compared to the plant size. Also, the Cerro Dominador hybrid power plant (see Introduction) employs a small battery for spinning frequency regulation only.

1.4 Hybridisation possibilities for Electricity Production

A CSP-PV power plant can be hybridised in several ways, achieving different "integration levels". Going from a lower integration level to an higher one, hybrid plants can be:

Grid-level integrated : in this case the power plant is seen as a single entity at the grid connection point, but there are no physical energy transfers between the main plant components. The integration consist in the application of different energy management strategies, varying the operation of the sub-systems according to external inputs and forecasts such as weather, electricity demand curve, market prices.

In this regard, Cocco et al. [48] synthesised two main options respectively named "P-INT" (partial integration srategy) and "F-INT" (full integration strategy). The P-INT strategy provided that the CSP and PV systems operated independently each other but keeping a single power delivery point, each working at an imposed and fixed share of the plant power production

profile. The F-INT strategy instead, provided for a synergetic operation of the CSP and PV systems to supply the required power output. In this case the control system optimised the shares of CSP and CPV power production.

The results showed that the F-INT strategy "leads to an effective use of the dispatch capabilities of the CSP plant owing to the presence of the TES section, while the CPV plant is fully exploited, especially during the hours of high solar radiation". In particular, being economic parameters not included in the work, the plant simulation achieved "better performance in terms of annual energy production and hours of potential time duration with fixed power outputs".

Examples of grid-level "fully-integrated" CSP-PV hybrid power plant are the recently-built Cerro Dominador in northern Chile (see Introduction) [19], the Ottana CSP-CPV pilot power plant [20], the Partanna small-scale CSP-PV hybrid [49].

Technology-level and grid-level integrated : Hybrid power plants can reach higher integration levels by enabling energy transfers between the different sub-systems, so that the energy management system can deal with more degrees of freedom and eventually achieve a better optimal solution.

Analysing the case of the CSP-PV hybridisation, the most straightforward way to enable an energy transfer between the two main sub-systems (namely PV and CSP) is to include an Electric Heater (EH) to convert some of the PV (or BESS, if present) output power into heat to be transferred to the hot HTF. The efficiency of the EH can be assumed ≈ 1, however, it must be noted that this transfer still represents a form of energy degradation. For this reason, in order to valorise the transferred heat and reduce the exergy destruction, it is important that the receiving HTF is as hot as possible, also being the PB able to achieve higher efficiencies with higher TIT. Riffelmann et al. [50] have recently investigated different design and operation options, corresponding to different integration levels, all based on molten salts as HTF, finding that for a site in Spain with mediocre direct solar irradiation the scenario with the lowest LCOE is the one employing an EH to charge the TES when appropriate. Also, Gedle et al. [51] economically compared two possible PT-oil-based hybrid plants in Morocco with different feed-in tariffs, one with an EH used as HTF temperature booster and one without it, obtaining an electricity cost advantage of almost 20% for the first option, regardless the different assumed feed-in tariffs.

In order to further improve the thermodynamic performances of a electricity-to-heat energy transfer, an alternative would be to install a heat pump instead of the EH. Indeed, heat pumps typically boast higher performances (COP>1), having as a drawback an higher cost and lower reliability. Mahdi et al. [52] recently researched on the possibility of integrating this kind of machines, specifically High Temperature Heat Pump (HTHP)'s, in a PT-oil-based CSP-PV plant in order to reach 565°C in the hot TES. In their work they pointed out that nowadays only heat pump systems Rankine gas compression cycle-based with maximum outlet temperatures of 165°C are

available on the market. Also, these commercially distributed systems are designed for operation with comparatively small temperature differences of less than 100°C. Instead, Brayton cycle HTHP's for temperatures up to 565°C are not yet commercially available, although these systems have drawn attention in recent years [53].

In future, a further step in the technical integration could be provided by the development of the compact CSP-PV concept. This hybridisation model would exploit the heat caused by the solar radiation not absorbed by the PV cells and by the various losses, rather than using and degrading electricity produced by PV. In this regard, in 2017 Ju et al. [54] presented an extensive review of the hypothesised or under development technologies. Other studies in this regard have been conducted by Otanicar et al. [55], focusing on the theoretical efficiency of such systems. According to Ref. [54], CSP-PV compact systems could greatly improve the overall generating efficiency, if solutions such as PV-topping or Spectral Beam Splitting (SBS) are implemented. However, these proposals entail much more technical challenges compared with the non-compact PV-CSP hybrid systems (i.e. the ones discussed in the rest of this thesis work), and no projects or prototypes of the compact CSP-PV were reported at the time the article was published. One main issue is the limited PV operating temperature, which soon induces premature components degradation and a strong efficiency reduction, allowing the generation of "poor" low-temperature heat only. A possible solution to that is the SBS, which reduces the solar cell temperature at same irradiation levels. However, a large part of radiation received by PV cells is still dissipated as heat without further utilization. Moreover, because of the high complexity of the system, there was also no prototype-level research on the SBS CSP-PV hybrid system at the time the article was written. Finally, the article reports a possible even more sophisticated yet more efficient solution combining together PV-topping and SBS.

As mentioned in the Introduction, to the author's knowledge the commissioned extra-large-scale Noor Midelt in Morocco is currently the sole practical example of a CSP-PV plant integrated also at technology-level, which includes a battery and a TES electric heater named "eTES" system [21].

Another possibility can be found in the increasingly popular concept of distributed virtual power plant. A virtual power plant is a network of decentralized, power generating units, as well as flexible power consumers and storage systems. All of these cooperate reducing possible stresses on the grid, and significantly increasing the system flexibility with respect to the single entities taken alone. Applying this concept to CSP-PV hybrid plants allows to delocalise the PV arrays from the specific site. In a context like Italy, this would help to bypass the often binding limit of a large-enough plot of land, having as only requirement the connection of the different sub-systems to the same local medium-voltage substation.

Chapter 2

Review of the optimisation methods

Exploring the literature regarding the optimisation of design and/or operation of hybrid energy systems, with particular focus on CSP-PV, it can be noted that various optimisation methods can be adopted for the solution of the problem. In this case also, as for the possible technical choices, there is no "silver bullet" solution, but rather each method is characterised by pros and cons, such as computational burden, flexibility, guarantee of convergence to global optimum.

Heuristic "greedy" algorithms : This kind of algorithms is typically used when the computational cost of determining an optimal solution is too high; it is a simple and "intuitive" approach. More specifically, a greedy algorithm is one that makes choices based on what looks best at each stage. In other words, choices are locally optimum but not necessarily globally optimum. Furthermore, a Greedy algorithm does not typically refine its solution based on new information. Plant operating strategies adopted in Ref. [42] and Ref. [14] are examples of such strategies. Both of them define the dispatch strategy starting from the electric power demand and power produced by solar field and PV as inputs, determining instant by instant how to operate the different energy flows based on a pre-determined flow diagram.

Mixed Integer Linear Programming (MILP) : MILP problems key elements is an objective function to be minimised (or maximised) subject to constraints. They may be represented by the following formulation in terms of continuous and 0–1 (binary) variables:

$$\min\ Z = c^{\intercal}y + d^{\intercal}x$$

$$s.t.\ Ay + Bx \leq b \quad \text{(MILP)}$$

$$y \in \{0,1\},\ x \geq 0$$

where Z is the objective function, c, d and b are vectors of coefficients, and A and B are matrices of coefficients (the rows represent the constraints and the columns represent the variables of the problem) [56]. The variables can be continuous (x) or binary (y), with the last ones serving to model the logical conditions (e.g. installation of a particular machines/subsystems in case of design problems, on/off of a particular machine/subsystem in case of operation problems). Mixed Integer Linear Programming is a technique

typically applied for the predictive operation planning or design of multi-energy systems. This approach can reach a good accuracy and achieve a high level of modelling details by introducing ad hoc constraints. Furthermore, once the problem is formulated as a MILP, it can rely on extremely fast and well-proven solution algorithms that guarantee the global optimality of the found solution [57]. Nevertheless MILP has characteristic drawbacks, especially when the design of a multi-energy system is considered: (i) nonlinear effects cannot be taken into account straightforwardly, requiring techniques such as piecewise linearisation, (ii) the necessity of considering all the time periods at once and the risk of high-dimensionality of the problem, which can be addressed through clustering algorithms aimed at temporal scale reduction by selection of typical periods and through rolling-horizon approaches [57]. Lamedica et al. [58] adopted a MILP methodology to optimize the sizing of PV-Wind renewable energy systems. Specifically with regard to CSP-PV hybrid systems, Hamilton et al. [43] have proposed solutions to improve the performances of MILP applied to the dispatch optimisation of a CSP-TES-PV-battery plant evaluated for two locations and two corresponding markets; Petrollese et al. [59] use MILP to model the scheduling different dispatch strategies affected by uncertainty.

Mixed Integer Nonlinear Programming (MINLP) : Given the drawbacks of MILP described above and an increasing number of applications that require the handling of nonlinearities, which in turn give rise to MINLP models, the development of such techniques has had several advances. However, MINLP algorithms suffer from lack of robustness of NLP solvers (no guarantee of finding an optimal solution, solver fails to converge) and from high computational expense for globally optimizing MINLP models [56]. As a consequence, an often-used approach is to reformulate the MINLP problem as a MILP one by using for instance exact linearisations of products of binary and continuous variables, or using piecewise linear approximations [56]. Powell et al. [60] performed the dynamic operation optimization of a hybrid solar thermal and fossil fuel system with NLP techniques. The objective function chosen was designed to minimize the total supplemental and pumping energy needed, while maintaining a constant total heat output for 24 h. Three degrees of freedom were identified at each time instance (corresponding to three independent mass flow rate streams). To reduce the dimensionality of the problem, the time horizon was discretised into smaller increments so that the solution had a finite number of decision variables. Hence, the 24 h time horizon was discretised into 15min increments, during which, each decision variable (flow rate) is held constant. The optimization problem was then solved "using standard Nonlinear Programming (NLP) solvers."

Genetic algorithms : The idea behind Genetic algorithms to which they are inspired is the process of natural selection. Their approach is classified as is a metaheuristic and they belong to a larger class named "Evolutionary algorithms". Evolutionary and Genetic algorithms (GA) are usually applied to solve different combinatorial optimization problems. Compared to

other methods they turn out to be more flexible and they can handle the non-linearity of the objective function and constrains [61]. However, the convergence to a global optimum is not guaranteed. With regard to CSP-PV, Zhai et al. [47] implemented a "greedy" operation strategy and optimised the design of a hybrid plant with a genetic algorithm in Matlab®; Starke et al. [13] used the same software to perform a multi-objective optimisation of a CSP-PV plant running with a quasi-baseload profile, obtaining a 3D Pareto frontier to help the investor choose the plant configuration based on the preferred combination of LCOE, CF and specific investment cost. In particular, TRNSYS® and GenOpt® were used "to design the numerical experiments and build a performance database for each configuration." Then, the Matlab® environment was employed to read the databases generated, build a surrogate model and perform the optimization routine using a genetic algorithm.

Another aspect regarding the problem solution and the optimisation process is whether uncertainty factors are present in the inputs, and in this case to which extent take them into account. Indeed, in some cases, the optimality of the solution may be compromised in presence of these factors, for instance when errors in the forecast of the energy demand, or renewable production (i.e. weather forecast errors), or market prices are introduced in order to make the optimization outcomes more realistic.

To overcome these issues, until now different approaches have been proposed:

Deterministic formulations with reserve requirements account for the non-deterministic nature of the forecasts by introducing margins and reserve requirements on the generation capacity, or worsening forecasts data of renewable sources by some percent. Thus, during real time corrections, net demand deviations from forecasts are compensated by a surplus in the available system capacity [62].

Stochastic programming is a widespread methodology to estimate the probability of occurrence of a determined event by associating a probability distribution to each factor of the problem which is subject to uncertainty. Subsequently, different scenarios with different values of uncertainty parameters are solved and handled by the optimization model [63].

Robust optimization approach models the uncertainty as a mathematical space, defining all infinite potential realizations of the elements within the uncertainty set, regardless of their likelihood. The identified solution, therefore, is feasible for all possible realizations encompassed by the uncertainty space, ensuring the safe system operation [64].

Petrollese et al. [59] presented a comparison of the deterministic, stochastic and robust approaches applied to two different weather forecast services, to be implemented in the Energy Management System (EMS) of the CSP-CPV Ottana pilot power plant. The aim of the paper was to identify the best approach to deal with the solar energy uncertainty, setting as objective function the maximisation of

the revenues obtained from the electricity sales in a day-ahead market. As expected, both the stochastic and robust approaches increased the revenues of the plant and minimised the risk of occurrence of unmet energy with respect to the deterministic approach. In particular, robust optimization achieved highest profits when weather forecast was characterized by low accuracy and more distributed errors.

Dominguez et al. [65] implemented a MILP to maximise the profit of a CSP plant operating as a price-taker in a pool-based electricity market, choosing a stochastic approach to model the market uncertainty and a robust one for the solar resource availability. More specifically, the authors developed a methodology to build offering curves for a Concentrated Solar Power plant. More solutions are available depending on the determined via a robustness parameter, expression of the degree of conservatism of the solution, which sets up the level of deviation considered in the uncertain parameters representing the solar power input. The results obtained in the paper show that higher values of the robustness parameter correspond to lower expected profits. However, the lower the level of conservatism, the higher the probability of experiencing penalties due to offering higher power than what the CSP plant will be able to produce.

An interesting approach was presented by J. Usaola [66], which proposed a technology-independent method that aims to maximise CSP plant revenues by taking into account daily electricity prices in the Spanish context. A MILP deterministic approach was adopted. The author implemented an optimisation model with a 2 days time horizon. However, he highlighted that for market participation, "bids must be produced each day and as new and more accurate predictions (of market prices and solar radiation) are available, it is advisable to use these more recent and reliable predictions." For this purpose a two-step optimisation process similar to a rolling-horizon approach was implemented and tested, with the difference that there is no progression in time since the last instant of time horizon is kept fixed. In particular:

> in the first step, the optimisation is run for 48 h (days D+1 and D+2), with estimates of radiation and prices for this time, available at day D. In this step, the optimal level of the storage at the end of day D+1 is obtained. Then, a second optimisation process is run, with the boundary condition for storage at the end of day D+1. [66]

Chapter 3

Possible plant layouts analysed

3.1 General configurations

While the focus of the work is put on hybrid power plant configurations including CSP, TES, PV, BESS and EH, CSP-TES and PV-BESS configurations are analysed for comparison purposes, too.

3.2 Sizes

As the background of this thesis is the investigation of the feasibility and the possible benefits of installing such RES power plants in Italy, the sizes analysed are tuned accordingly.

Despite the economics of CSP plants generally benefiting from bigger sizes, thanks to improved performance of power components derived from traditional generation technologies and to scale economies [67], the Italian context imposes a different perspective. This is due to various reasons [68]: (i) the limited availability of contiguous and sufficiently smooth land plots wider than 150 ha in the areas in which sun irradiation is more abundant, such as southern Italy or Sardinia; (ii) the current Italian Feed-In-Tariff scheme does not allow the use of potentially polluting HTF's, such as synthetic oils, outside of industrial areas, whereas Solar Salts are allowed; (iii) Italy does not have vast, remote, desert uninhabited areas, therefore the environmental impact often becomes a very relevant matter. Condition (i) favours the linear fresnel technology against parabolic troughs and even more against solar towers, thanks to higher area-specific energy density; for what concerns the PV side of the plant, the same logic leads to the choice of a GCR near the typical upper bound found in literature, even though the PV field has the possibility of being delocalised, partially relieving condition (i), as outlined at the end of Section 1.4. Condition (ii) limits the application of the most traditional and well-studied thermal oil-parabolic trough. Condition (iii) again favours linear fresnel technology thanks to lighter foundations compared to parabolic troughs and solar towers, other than much lower visual impact, especially when compared to solar towers, because of the considerable height of the tower itself.

As a consequence of land area limits and rising social and environmental concerns moving towards bigger plant sizes, the PB size limits used in the optimiser are

10 $MW_{el,gross}$ as lower bound and 100 $MW_{el,gross}$ as upper bound. Moreover, the maximum TES size is imposed on 24 h and the maximum BESS size on 1000 MWh. Besides, the max land area considered is 150 ha, except in the case of delocalised PV.

Given that, firstly the solver is allowed to freely choose the best size of each component (within the above-mentioned limits and the model constraints) according to the selected objective function, so that the theoretical optimum can be reached. At a later stage, evaluating the results obtained in the free or "convex-hull" optimisation, the PB sizes are fixed to 10 $MW_{el,gross}$ and to 50 $MW_{el,gross}$ to simulate a "mid-small" plant and a "mid-big" plant respectively, according to the indications provided by ENEA.

3.3 Subsystems

Photovoltaic field : the most common large-scale technology is chosen in the simulations, employing multi-crystalline silicon modules with 17% Standard Test Conditions (STC) efficiency. The default mounting is fixed and the GCR set to 0.6, as introduced in the previous section.

Battery Energy Storage System : li-ion battery storage system, as discussed in 1.3.

Solar Field : Molten Salts Linear Fresnel and Solar Tower systems are compared, both using the more tested "Solar Salts" as HTF. The Molten Salts Linear Fresnel (MSLF) field uses Archimede HCEMS receivers [69] and FRENELL collectors [70] [71]; the Solar Tower uses SAM's engine with default values except for heliostats field size - tower height proportions taken from Cerro Dominador power plant. In addition, a MSPT with Archimede HCEMS receivers and 5.9 m wide collectors is only used for reference comparison in a part of the work aimed to model the behaviour and operation of linear Molten Salts Solar Fields

Thermal Energy Storage : the proven two-tank system is chosen, Solar Salts are used. This configuration, in combination with the selected Solar Fields, not only allows to store the HTF at temperatures up to 550°C, valorising the production surplus converted to heat by the EH as explained in Section 1.4, but also enables a "direct storage" solution (i.e. no HX's are required between SF and TES).

Power Block : Steam Rankine cycle technology, as it is the most common and established for the size range of interest, adapted and tuned in the software Thermoflex® to allow more flexibility and to avoid problems related to molten salts freezing. The power cycle is air cooled in order to increase the number of suitable plant sites.

Subsystems interconnections : according to the categorisation used in Section 1.4, the hybrid plants considered are technology-level and grid-level integrated. Specifically, they are operated with a "fully integrated" EMS and

include Electric Heaters in the TES, as widely applied in pilot systems by ENEA [72], and similarly to what is being done with the "eTES" technology in the Noor Midelt plant in Morocco [21]. Figure 3.1 shows the generic scheme of the proposed hybrid plants, outlining the main interconnections. As can

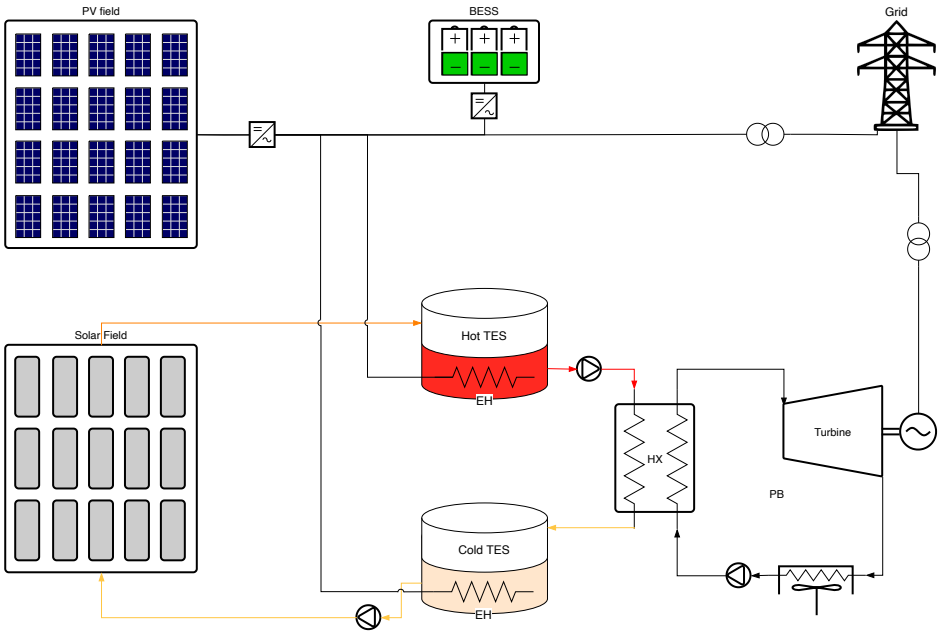

Figure 3.1. Generic scheme of the proposed hybrid plants

be noted, the Solar Field is directly connected to the tanks of the TES, while the Power Block exploits the HTF heat via the HXs of the steam generation system. Lastly the turbine electric generator is connected to a transformer increasing the voltage to the level required by the grid. As regards the PV side of the plant, AC coupling of the components has been chosen as it seems to be more proven and reliable [73, 74]. Hence, the output of the PV is always converted to AC, which is sent to grid through a transformer, to the Electric Heaters, or re-converted to DC when batteries need to be charged. Similarly, when the BESS is discharged for any purpose, its output is converted to AC. In case of delocalised PV field(s), the same logic applies, except for the fact that the AC electric output is firstly sent into the nearest Medium Voltage (MV) substation to be redirected either to the rest of the power plant or to the grid.

Chapter 4

Methodology and models

Having the defined the possible plant configurations and subsystems, a cautious modelling is required to evaluate the performances of the various plants analysed.

In this chapter, firstly "exogenous" models, built and/or pre-processed externally to the optimiser, are presented and described. Secondly, the k-MILP data clustering technique allows to understand how the exogenous profiles are introduced and treated in the MILP algorithm. At this point, the "endogenous" models, which are managed within the algorithm, are explained and the equations governing their behaviour are outlined. Once the different model components have been detailed, an overview of the optimisation options is provided and their functioning explained where necessary, concluding the part of this work dedicated to the "architecture" of the model. After that, the economic assumptions and data sources on which the model is based are introduced. Lastly, the bases and assumptions behind the testing of the model based on data from an existing hybrid CSP-PV power plant are outlined.

.-..... CHECK.....

4.1 Exogenous models

Given the complexity of the optimisation problem considered, especially in case the design of the power plant is investigated (i.e. the sizes of the subsystems are not fixed), the possibility of pre-processing some particular data to be used among the MILP inputs must be considered, thus reducing the computational burden of the simulations. Exogenous models are mainly provided to the optimiser in the form of data profiles, as extensively described below and in the following sections. Moreover, data obtained externally from Power Block simulations are conveniently pre-processed and "packed" through reasonable approximations, in order to be smoothly integrated in the plant model algorithm.

The exogenous profiles used as input in the MILP model are some 2-years long data series, discretised into 1h timesteps, in particular: electricity demand curve, power market prices, RES production profiles (obtained from weather data).

The choice of 2-years long profiles is the result of a trade-off.

On the one hand, if the design of a RES-based power plant is to be optimised,

Typical Meteorological Year (TMY)[1] should be used in order to avoid incurring in weather peculiarities happened in a particular year, which would cause an incorrect sizing of the power plant components. On the other hand, in some optimisation cases, the shape of the electricity demand curve or the power market prices must be taken into account. In these cases, a problem in the design optimisation arises. The weather, electricity demand, electricity market price are not independent. The last two are clearly correlated, high demand typically corresponds to higher price, but the weather has influences on them, too. For instance, a particularly warm day can cause an intensive use of air conditioning devices, increasing electricity demand and market prices as a consequence. However, the demand and the prices can be characterised by historical trends, even in the short-term, making the creation of "synthetic" typical years questionable for these profiles.

Hence, the most recent 2 years period available, in combination with clustering techniques (see Section 4.2) has been selected as a good compromise between weather peculiarities (that could be particularly influencing if a single year was used), historical trends of the electricity demand and electricity market prices (that would be more evident in case of a 5-10 years period), and computational time required by the clustering algorithm.

As a note, the plant design could be optimised using the TMY for the generation of RES profiles in the following case: pre-determined production profiles not dependent on actual electricity demand and pre-determined electricity revenue profiles as in the case of some particular incentive schemes.

Besides the weather, electricity demand and market prices, RES production profiles are generated exogenously as well, on the basis of the weather ones. Indeed, sun-dependent subsystems are not dispatchable if taken alone, so the optimiser cannot significantly act on them, or even possibly it would add too much complexity and non-linearities not manageable by the MILP. Therefore, a priori "greedy" optimisation strategies are adopted for the operation of these subsystems. The output of such models, detailed in the following sections, is taken specific to the area, so that the optimiser can decide "how much" of each technology to install within the system boundaries and constraints, if the design option is activated.

4.1.1 Weather, electricity demand, market price profiles

Weather data are used as input for the RES models described in the sections below, in turn, the output of those models are given in input to the MILP optimiser. Electricity demand profiles and market prices (when needed) are instead provided directly to the MILP.

Weather data

The Weather data used for the approximate project location - a well-insolated area in Italy - has been provided by ENEA for the location of Priolo Gargallo, Sicily. In particular, the TMY is used for specific subsystem design purposes only, as described in Sections 4.1.2 and 4.1.3, while for the whole plant optimisation

[1]Data containing actual weather sequences that represent the mean long-term climatic conditions for a particular location.

2 years-long weather data from 2016 and 2017 (the most recent available) has been used, as explained in Section 4.1. Moreover, in order to test the correct functioning of the optimisation algorithm, the model has also been run with input data characterising the existing Cerro Dominador power plant (see Section 4.6). In this case the weather file used as input has been retrieved from the Chilean Ministry of Energy's website "Explorador Solar" [75], which provides the TMY for a selected location, calculated from models based on satellite-derived data. As a note, the TMY can be used in this particular simulation since it has been assumed that the Cerro Dominador plant operates following an almost constant output profile (see Section 4.1), which is a fair assumption, given the abundant solar radiation of the location, the maximum Power Purchase Agreement (PPA) yearly volume the project secured [76] and the statements Abengoa made in presentation material regarding the project [77].

Table 4.1 provides a summary of the irradiation parameters of weather data used in this work.

Table 4.1. Weather data summary

Weather Data	DNI [kWh/m^2/y]	GHI [kWh/m^2/y]
2016-17 Priolo	1770	1702
TMY Priolo	1847	1730
TMY Cerro Dominador	3715	2561

It can be noted that the most recent 2 years-long weather data available shows lower irradiation values compared to the TMY, so its usage will lead to more conservative estimates in the plant model optimisation.

Electricity demand profiles

Different options of electricity demand profiles can be chosen in the proposed model, according to optimisation objectives and investor requirements.

Firstly, demand profiles can be either pre-determined or optimised.

Secondly, as regards the shape of the profiles, they can be either constant or national-demand shaped. The latter has been chosen instead of the Sicilian one in order not to loose generality.

- **Pre-determined demand profiles**
  - **Constant**: in this case the plant is asked to introduce into the grid a constant amount of electric power, set a priori, e.g. 50 MW_{el}.
  - **National demand-shaped**: in this case the 2016 and 2017 Italian electricity demand curves are rescaled according to pre-determined logic, e.g. the peak value of the profile equal to the maximum output power of the PB, or the cumulative of the demand equal to the energy produced by the power block if run at nominal conditions for the whole year. Hence, the hybrid plant is asked to provide to the grid a time-varying amount of power, according to the demand profile.

- **Optimised demand profiles**
  - **National demand-shaped - optimised "globally"**: in this case, the original 2016 and 2017 Italian electricity demand curve is rescaled according to a single parameter (a multiplicative factor) hereby referred to as "k", chosen by the optimiser.
  - **National demand-shaped - optimised "period by period"**: in this case, the original demand curve provided as input is optimised rescaling it with different multiplicative factors "k_i", one for each period (see Section 4.2 - k-MILP Clustering).

Figure 4.1 shows the Load Duration Curve (LDC)[2] of the Italian electricity demand for years 2016 and 2017.

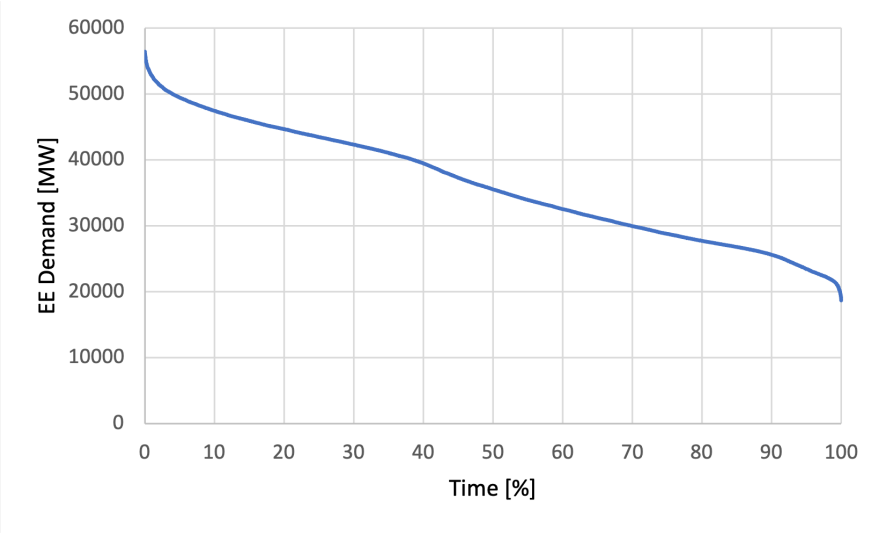

Figure 4.1. Load Duration Curve for years 2016 and 2017

Power market price profiles

Depending on the option selected in the optimiser, electricity market prices may be considered if the objective is to maximise the profits of the plant.

Again, the market price considered is the "Prezzo Unico Nazionale (PUN)", which is the reference price for electrical energy recorded on the Italian Power Exchange (IPEX), so as not to loose generality.

Different options are available also for the electricity market profiles:

- **Most recent Italian incentive scheme**: the most recent formula for the calculation of the state incentive for a hybrid CSP power plant is the following [78]:

$$Incentive\,(I) = Base\,tariff\,(Tb) + Prize\,(Pr) - Zonal\,price\,(Pz) \quad (4.1)$$

  where:

[2]LDC: in this curve data is ordered in descending order of magnitude , rather than chronologically

Tb = 291 €/MWh (valid for plant sizes bigger than 5 MW);

Pr = 45 €/MWh, since the power plant considered belongs to the category "supplementation fraction[3] up to 0.15";

Pz is assumed equal to the PUN for the reasons described above.

As a result, in this case whenever electricity is sent into the grid, a constant revenue of 336 €/MWh is guaranteed, and according to the regulation it will be granted for 25 years.

This reward is subject to some constraints, though. The plants need to have a TES greater than 0.4 kWh_t/m^2 if the aperture is between 10,000 and 50,000 m^2, or greater than 1.5 kWh_t/m^2 if the aperture is larger than 50,000 m^2. Moreover, as outlined in Section 3.2, toxic or harmful HTF's, as thermal oils, cannot be used, except in industrial areas.

- **PUN rescaled**: in this case the PUN profile is rescaled with a pre-determined multiplicative factor, e.g. so that the average modified PUN price is equal to $Tb + Pr$.

Figure 4.2 shows the "PUN Duration Curve" of the Italian electricity market for years 2016 and 2017.

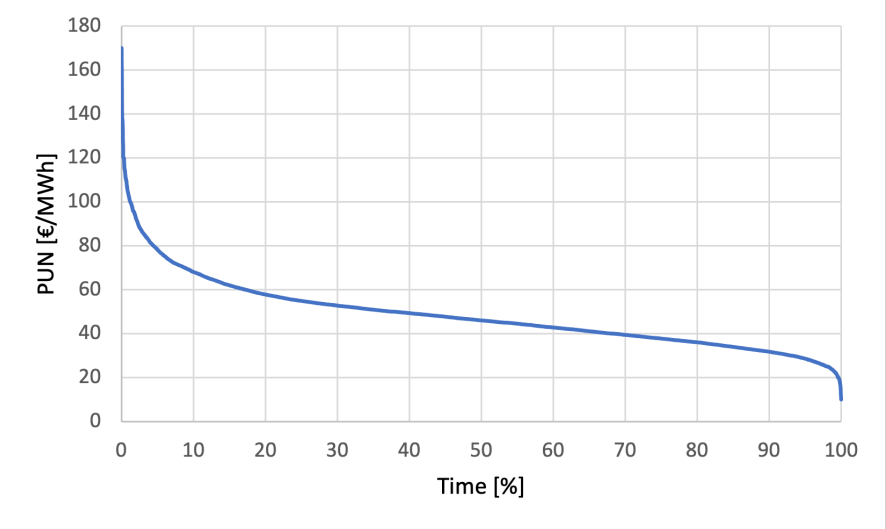

Figure 4.2. "PUN Duration Curve" for years 2016 and 2017

4.1.2 PV model

Choosing a fixed-mounting PV, the only parameter of this part of the power plant that can be optimised in the MILP is the amount of modules installed, thus the area and the nominal power of the array(s). However, the power profile provided as input to the MILP is subject to a preliminary design optimisation.

[3]Supplementation fraction: the net production quota not attributable to solar source.

The two main parameters related to the design pre-optimisation of the PV field are the tilt angle of the modules and the GCR of the array(s). The azimuth, which is the angle that determines the array's east-west orientation (as in a compass), is assumed equal to 180°, being the optimal condition in the northern hemisphere an array facing south. This value should be changed only in case of shading caused by hills, trees, other objects on the horizon, or in case of particular constraints imposed by the shape of the plot of land chosen.

The tilt angle and the GCR values are not independent, indeed, a particular GCR corresponds to a particular optimum tilt angle. This interdependency is caused by the self shading that happens between the rows of the array, especially when the sun altitude angle is lower. Tighter modules rows (higher GCR's) are more penalised by self-shading effects than looser ones. Hence, higher GCR's are associated with lower tilt angles, because the incoming radiation when the sun is at low altitude values cannot be exploited effectively in this case.

Beyond that, the tilt angle can be optimised according to different objectives:

- maximisation of the yearly energy yield
- maximisation of the summer energy yield
- maximisation of the winter energy yield

The "classic" yearly energy yield maximisation has been chosen as base case. Further details and explanations in this regard can be found in

The tilt angle has been optimised using the "Detailed Photovoltaic Model" in SAM, using the TMY for the selected location (Priolo Gargallo, Sicily) provided by ENEA (see The detailed model has been chosen since, even though it requires a more complicated setup, it has returned results more in accordance with typical self shading loss values for similar locations and GCR found in literature.

Also, the SAM model has been tested with a simplified spreadsheet model developed in-house for comparison purposes. The latter takes as input the same TMY, accounting for beam, diffuse radiation and albedo, temperature and wind. Firstly, the sun position is accurately calculated according to the geographical coordinates of the location and to the equation of time, then geometrical relations allow the calculation of the incidence angle on the modules surface. Sky and ground view factors, which are dependent on the tilt angle, are calculated as well, so that eventually the total radiation G_T hitting the PV surface can be obtained. Based on G_T, ambient temperature and wind speed, the operating cell temperature can be estimated using the Nominal Operating Cell Temperature (NOCT) method reported in the following equation [79]:

$$T_C = T_{amb} + (T_{NOCT} - T_{amb,NOCT}) \frac{G_T}{G_{T,NOCT}} \frac{U_{L,NOCT}}{U_L} \left(1 - \frac{\eta_{PV,actual}}{\tau\alpha}\right) \quad (4.2)$$

where:

T_{NOCT} is the nominal operating cell temperature provided by manufacturers;

$T_{amb,NOCT}$ is 20°C;

$G_{T,NOCT}$ is 800 W/m^2;

$U_{L,NOCT}$ is the heat transfer coefficient at the NOCT conditions and is equal to 9.5 W/m^2/K;

U_L is the heat transfer coefficient at the actual conditions in W/m^2/K equal to $5.7 + 3.8\, v_{wind}$;

$\tau\alpha$ is the transmittance-absorptance coefficient assumed equal to 0.8.

Finally, the calculation of the actual efficiency (equation 4.3),

$$\eta_{PV,actual} = \eta_{STC}\,[1 + \gamma\,(T_C - T_{STC})] \tag{4.3}$$

where:

γ is the power temperature coefficient assumed -0.4%/°C according to typical values for silicon-based cells;

T_{STC} is 25°C.

which depends on the cell temperature T_C, is the last step towards the calculation of the DC power produced. Two unknowns (T_C, $\eta_{PV,actual}$) are involved in the above-written equations 4.2 and 4.3, generating an easily solvable system of linear equations. The results returned are coherent, showing the same order of magnitude. As expected, the simplified model calculates moderately higher production values, since, as instance, it does not account for different actual absorption of the beam radiation at different incidence angles ($\tau\alpha$ is not constant) and neglects self shading between rows.

The DC output profile used as base case input for the MILP has been obtained using the input parameters listed below, following the above-mentioned optimisation:

- GCR: 0.6
- Tilt angle: 26°
- multi-crystalline silicon module from SAM CEC Performance Module Database:
  - η_{STC}: 17.14%
  - γ: -0.415%
- DC losses:
  - Module mismatch: 2%
  - Diodes and connections: 0.5%
  - DC wiring 2%
  - Nameplate 1%
- Soiling loss: 5%

The DC losses assumed correspond to the default values of SAM, except for Namplate assumed 1% instead of 0% in order to obtain a more conservative estimate. Additionally, given the relevant performance degradation to which PV modules are subject in time, mainly as a consequence of exposure to ultraviolet radiation, a 0.6%/y output drop has been considered [80]. Since the MILP model optimises the design simulating 1 year of operation only, the generated PV output profile has been multiplied by a degradation rate considered as if the modules were at half of the plant lifetime, so:

$$E_{PV,degr} = E_{PV}\,(1 - d_{PV})^{\left(\frac{lifetime}{2} - 1\right)} \tag{4.4}$$

(more detailed model should account for degradation in time... o alternativamente prendere qui un valore medio (83% ca. a 25 anni da datasheet)

The generated profile, which takes as input the weather data of years 2016 and 2017 in Priolo Gargallo (see Section , is then normalised with respect to the active surface in order to let the optimiser choose the best amount to be installed.

4.1.3 Solar Field models

Linear technologies : In the case of linear Solar Field technologies, owing to the reasons explained below in this section, it has been necessary to develop a dedicated Matlab® algorithm in order to better account for the different modes of operation.

The developed SF model takes as inputs the DNI from a weather file and the sun position-dependent part of the optical efficiency, the latter being generated by the widely used SAM software developed by NREL [81], which in turns needs as input the "Collector incidence angle table" in the case of MSLF [82], or the collector model in case of MSPT. The output provides timestep by timestep or EDNI by EDNI the loop mass flow rate, the loop outlet temperature, the heat absorbed by the HTF, the loop pumping power, binary variables that indicate the operation mode to be read by the MILP model.

The SF loop is discretised in equal sections about 5 m long, so that the algorithm calculates the input and output values section by section till convergence to the required temperature or mass flow rate is reached. In order to estimate thermal losses from the "active" (i.e. receiving the concentrated solar radiation) part of the receiver, discrete values of heat losses have been taken from the brochure of the Archimede receiver [69], then the Excel function LINEST has been used to obtain a polynomial regression of the datapoints. The chart obtained in Figure 4.3 corresponds to the one ENEA reported in [83] adopting the same receiver tubes. In the Matlab® code, the polynomial expression of the heat losses

$$\dot{Q}_{loss,th} = 1.629\,63\text{e}{-5}\,T^3 - 0.01278\,T^2 + 4.37910\,T - 504.12698\ [\text{W/m}] \tag{4.5}$$

has been integrated section by section in order to obtain a more accurate evaluation. Then, a 1.2x multiplier has been added in order to account for

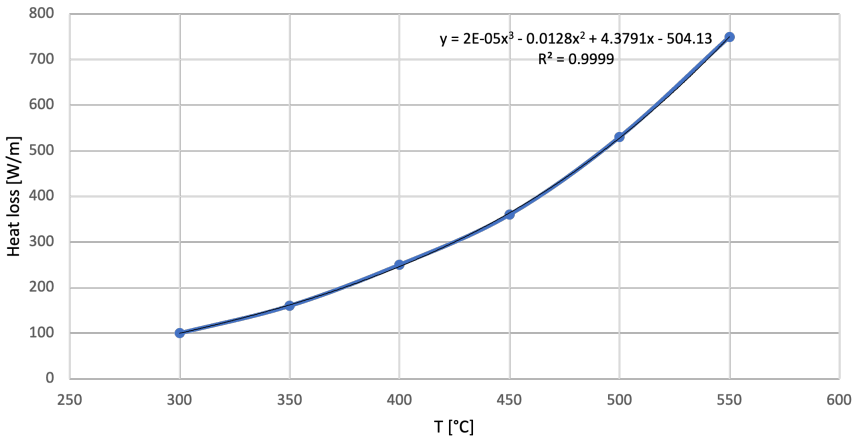

Figure 4.3. Length-specific heat loss from receiver tube

losses from "non-active" parts of the loop. The 1.2 value has been obtained tuning the model with the reference provided by ENEA, in which they simulated a complete string including all its components [83]. Also, section by section the following energy balance must be respected:

$$\Delta l \, (EDNI \; w \; \eta_{opt,nom} - \dot{Q}_{loss,th,i}) = \dot{m}_{loop} \left[h_{out,i} + \frac{v_{out,i}^2}{2} - \left(h_{in,i} + \frac{v_{in,i}^2}{2} \right) \right] \tag{4.6}$$

where:

Δl is the section length;

w is the active width of the collector;

$\eta_{opt,nom}$ is the nominal optical efficiency, or the part of the optical efficiency which does not depend on the sun position

h : the static enthalpy is calculated according to the following equation valid for Solar Salts in their temperature operating range:

$$h_{x,i} = \int_{T_{ref}}^{T_{x,i}} c_p \, dT = \int_{T_{ref}}^{T_{x,i}} (1443 + 0.172 \, T) \, dT \tag{4.7}$$

The balance is used in the algorithm calculation loops in order to obtain the temperatures and/or mass flow rates, according to the operating condition of the Solar Field.

In order to obtain the loop pumping power it is necessary to calculate the loop pressure drop beforehand. This last one is calculated summing the pressure drops of all the sections, which are in turn obtained from the Darcy-Weisbach equation, with the friction factor calculated from the Churchill correlation, using a value of 1.5e−6 m as pipe internal surface roughness. Having the Δp of the loop, the following equation estimates the pumping power:

$$\dot{W}_{pump,loop} = \dot{m}_{loop} \frac{\Delta p}{\rho} \frac{1}{\bar{\eta}_{pump}} \tag{4.8}$$

$\bar{\eta}_{pump}$ is assumed constant and equal to a more conservative value of 0.75 to account for off-design operation.

ρ is the density of the HTF at the SF inlet temperature (assumed 290°C, except in case of recirculation), since the SF pump(s) are installed upstream the SF itself.

The loop pumping power is then used to estimate the total SF pumping consumption in the optimiser, multiplying the single loop value by the obtained number of loops.

Linear technologies have the HTF flowing in piping significantly exposed to ambient temperatures, so that particularly in case molten salts are used, warm-keeping recirculation is necessary to avoid formation of cold spots and freezing in the SF pipes. In addition, even though not implemented in the proposed model due to computational reasons, the real-world models of molten salts-based linear CSP plants include heat tracing on joints, valves and other "non-active" (i.e. not receiving the concentrated solar radiation) components, and "Joule heating[4]" in the "active" receiver sections. However, these two modalities should be used just in case of very prolonged absence of solar radiation or in situation as start-ups required by maintenance operations.

Moreover, given the relatively high nominal temperature of Solar Salts, the Solar Field cannot guarantee sufficient heat on the receiver piping so that to reach 550°C at all times during daytime. That happens both as a result of receiver thermal losses and because of the loop[5] mass flow rate lower bound set by the necessity of achieving turbulent flow in the piping, thus improving the heat transfer coefficient. As a result, in that situation two options are possible: sending the SF output to the hot tank, reducing its temperature with respect to the nominal conditions; sending the SF output to the cold tank. In order to avoid downgrading the energetic state of the hot tank of the TES or sending colder fluid to the Power Block Heat Exchanger with a consequent reduction of the cycle efficiency, a recirculation of the HTF in the Solar Field is possible. (RESTO a riguardo, why not recirc, res&disc) (Figure ....(a) and (b) depict the SF-TES subsystem w/ and w/o recirc)

Given what above, four operating conditions of the SF-TES subsystem have been identified (modes 3a and 3b refer to the configurations with and without recirculation, respectively). The model has been developed hypothesising a constant SF input temperature of 290°C. This corresponds to assuming a cold TES outlet temperature equal to 290°. Though this might be not true, the MILP processing the data obtained with the Matlab® model is not able to take temperatures into account accurately because of non-linearities that would otherwise arise, so the benefit of including variable SF temperatures would be vanished in a second stage.

[4]Joule heating: in this context, the expression refers to heating performed by means of direct injection of DC or AC current directly into the receiver pipes, exploiting the steel electrical resistance to produce heat [68].

[5]Solar Field loop: a series of SF modules. A Solar Field is usually composed by more loops in parallel.

1) **Solar Field warm-keeping (SFwk)**: this modality is activated when the EDNI is not sufficient or null, causing the cooling of the Solar Field. As a consequence, the SF is drawing energy from the cold TES, taking HTF stored in it and returning it colder. In case the SF loop output temperature would fall below 275°C, an increase in the loop mass flow rate with respect to the minimum setpoint is needed in order to prevent that from happening.
2) **Power to cold tank (P2TESc)**: from the plant control point of view, this operating mode basically corresponds to the cases of SFwk in which it is not needed to increase the loop mass flow rate. However, it is different from the model point of view for the fact that in this case the SF is partially heating up the HTF, hence increasing the cold TES internal energy rather than reducing it. The loop mass flow rate is fixed at the minimum setpoint.

3a) **Power to hot tank (P2TESh)**: for EDNI values over a certain threshold (which depends on the technology considered - MSLF or MSPT - and on the loop length) the loop outlet temperature reaches high enough values so that the heated HTF can be sent to the hot tank without significantly affecting the tank temperature. The outlet temperature at which this operating mode is activated has been set to 440°C (as it resulted a good compromise after some tests... res&disc). The name has been chosen as opposed to P2TESc to highlight the switch of the HTF flow destination tank (bypass active in this case?). The loop mass flow rate is still kept at the lower bound to achieve the maximum possible outlet temperature.

3b) **Solar Field recirculation (SFrec)**: In case recirculation is implemented, over a certain EDNI threshold, keeping the loop mass flow rate fixed at the lower bound, the nominal loop outlet temperature (550°C) can be reached. Hot HTF exiting the loop is partially sent back at the loop inlet, so that the average loop temperature is higher and the objective can be achieved. The output loop mass flow rate is reduced depending on the amount that needs to be recirculated in order to reach 550°C at the outlet, according to the following simple mass balance:

$$\dot{m}_{out,t} = \dot{m}_{loop,t} - \dot{m}_{rec,t} \tag{4.9}$$

where:

$\dot{m}_{out,t}$ is the loop outlet mass flow rate to be sent to the hot tank or to the PB HX;

$\dot{m}_{loop,t}$ is the mass flow rate circulating in the SF loop;

$\dot{m}_{rec,t}$ is the loop mass flow rate recirculated;

4) **Nominal**: In the "nominal" case, the loop operating outlet temperature is set to the maximum value at which the receiver has been successfully tested (i.e. 550°C) [69]. In order to respect this constraint, the loop mass flow rate is increased in proportion to the EDNI.

The algorithm for the linear SF simulation has been validated both with (i) SAM software and with (ii) a reference document from ENEA in which the operation of a molten salts-based MSPT plant has been simulated [83]. In particular, (i) the yearly net produced power by a loop, area-specific, has been compared with the SAM output values "HTF absorbed power" subtracted of "Field Thermal Power Header Pipe Losses", obtaining a relative error of about -6%, possibly due to approximations in the Matlab® model such as neglected thermal inertia of the system, and different operation strategies compared to SAM, which for instance uses electric heaters instead of increased mass flow rate in case of very low EDNI. (ii) the paper from ENEA reported a chart showing the values of loop mass flow rate and loop outlet temperature against EDNI for a MSPT using an Archimede receiver with an internal diameter of 0.064 m [69], parabolic mirrors 5.9 m wide, with 75.6% nominal optical efficiency, 576 m loop active length. Using these same inputs in the Matlab® model returned the same values found in the chart by ENEA. The plot obtained is reported in Figure 4.4

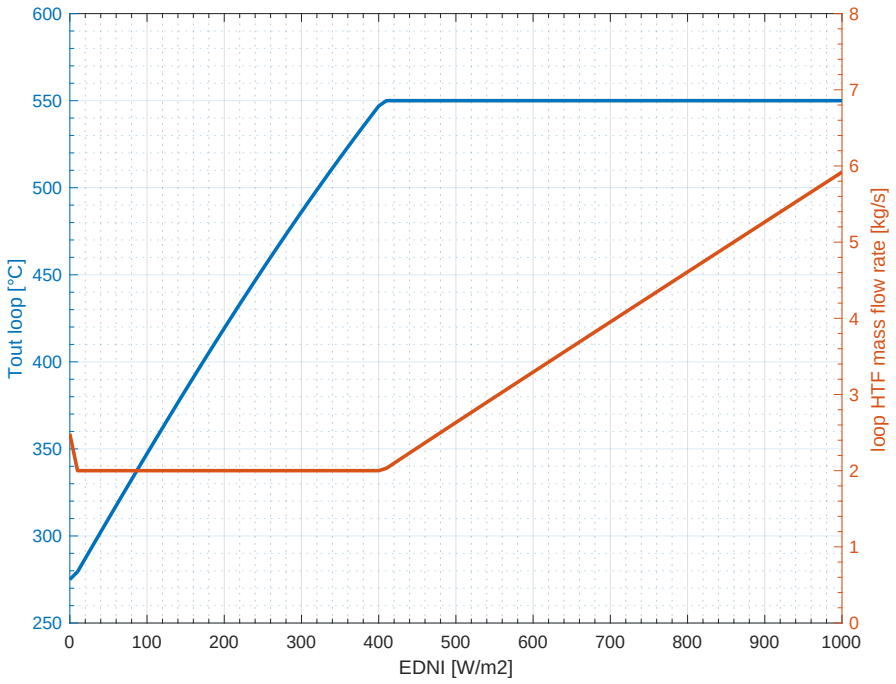

Figure 4.4. Main MSPT Solar Field operating parameters at different EDNI's

In addition, a separate version of the Matlab® model has been developed in order to preliminarily assess the appropriate SF loop length according to the EDNI "LDC" processed from the TMY of the selected location.

Point-focus technology - Solar Tower : In the case of Solar Tower, given the lower relevance of the above discussed issues, the production profile is taken from SAM. As already outlined previously, the MILP model needs as input area-specific RES production profiles, so that in case the design is to be optimised, the land area to be equipped with PV or SF can be chosen by

the optimiser. However, differently from linear technologies, which can be approximated to modular with a fairly low error (i.e. square meters of SF can be added without significant scale effects on behaviour and performances), Solar Towers performances are influenced by the size of the heliostats field and by the tower height, which is in turn connected to the heliostats field area. This behaviour is mainly ascribable to variations in the optical efficiency due to the increased weight of atmospheric attenuation and "spillage[6]" losses, given the increased heliostat-receiver distance with increasing sizes. Nevertheless, given the sizes investigated in this work, which in the case of Solar Tower-based CSP plants vary between 10 and 50 MW_{el}, the results in terms of nominal PB input power / aperture area ratio (at a fixed typical Solar Multiple (SM) of 3) obtained from SAM for the selected location did not show significant differences, considering the whole model context. Thus, the production profile used as input for the MILP in case of Solar Tower has been chosen as the one simulated with a mid-range (approx. 30 MW_{el}, SM=3) size, dividing it by the simulated aperture area. Moreover, it must be noted that in order to generate the optimum heliostat field layout, coupled with the optimal tower height and receiver size, the TMY for the selected location has been used. Still in SAM software, the max. and min. "heliostat distance to tower height ratio" parameters in the SAM software have been set to 6.6 and 0.6 respectively, according to what has been done in the Cerro Dominador power plant. These parameters are involved in the generation of the optimal heliostats field and in its GCR.

4.1.4 Power Block model

The "core" of the Power Block models has been developed with the software Thermoflex® and is not object of this work. However, data obtained from those simulations need to be post-processed in order to be fed to the MILP in a convenient way. Indeed, different Power Block sizes not only are characterised by different operating ranges, but also by different efficiencies. In this regard, the present section describes how the above-mentioned convenient expression to be used in the MILP can be obtained.

Firstly, it must be pointed out that the PB operating curves described below are obtained at a constant nominal ambient temperature $T_{amb,PB} = 30°C$ and .....% Relative Humidity (RH) (these parameters affect the air condenser operation, hence the PB performances), for the sake of simplicity.

Thermoflex® simulations have been run at discrete size (20-100 MW) and input load fraction (20%-100%) intervals, so as to obtain various data series. In particular, for each size and for each input load fraction, the relevant parameters are: thermal power input [MW_{th}]; net power output [MW_{el}]; net efficiency, which can be simply calculated as the ratio between the other two quantities. Figure **??** shows the net power output against the thermal power input for some different PB sizes.

Applying a multiple linear regression on the data series presented in Figure **??**,

[6]Spillage losses are related to reflected energy that does not hit the receiver because of tracking errors and imperfect mirror surface.

allows to obtain the coefficients (K_1, K_2, K_3) of a linear approximating function (see equation 4.10), originally developed by Yokoyama et al. [84], which links the input and the output of the PB, obtaining different values depending on the size of the machine itself.

$$P_{el} = K_1 \dot{Q}_{th,in} + K_2 S + K_3 \tag{4.10}$$

Where:

P_{el} is the output net electric power [MW_{el}];

$\dot{Q}$ is the input thermal power [MW_{th}];

S is the size of the machine in terms of input thermal power [MW_{th}].

K_1, K_2, K_3 are linear coefficients, which respectively account for [84]: (1) a constant efficiency for any PB, if load and size dependencies were neglected; (2) the part-load efficiency variation for a fixed size unit; (3) the size effect on efficiency. The expression can then be easily implemented in the MILP.

Power Block warm-keeping model

A parallel exogenous model, still related to the PB, but also to the Solar Field, has been developed in order to account for the heat losses attributable to the need to keep the molten salts side of the steam generation system warm enough in order to avoid salts freezing.

It has been hypothesised / assumed... + PB warmkeeping, connected to steam generation system, binary vairable, modello tubo.... in HX assumed no losses or gains (water stagnata li) to eco maybe loses but acquires from SH (RH) and EVA

In heat loss correlation Tamb assumed equal to average T throughout the whole period considered, should be a conservative estimate as the PB more often runs during night when PV is OFF (check this hypothesis), so T during day when wk happens is higher. ....

4.2 k-MILP Clustering

As mentioned in Chapter 2, in the MILP formulation, if the design is to be optimised, the design problem and the scheduling problem are tackled simultaneously. Given the complexity of the system, this results in a very large number of variables and constraints, thus making the problem very challenging from the computational point of view. In this case, a workaround is provided by the "clustering technique", which allows a dimensionality reduction by selecting a series of representative or "typical" periods, instead of the whole year or period considered.

In this thesis work, the clustering is made via the "k-MILP" algorithm, a code that allows the selection of a certain number of typical and "extreme" periods, based on multiple input profiles [84].

Compared to the mostly used k-means, which creates synthetic representative days as arithmetic averages of each cluster and tends to smooth the profiles, or k-medoids, which picks up a real day from each cluster and tends to result in

discrepancies between the aggregated and the original LDC, the MILP model-based k-MILP relies on the k-medoids method but ensuring that the original LDC is preserved within a certain tolerance, where required [85]. Comparative results have shown that k-MILP is a valid alternative to the above-mentioned well-known clustering techniques.

The length or duration of the clustering periods can be chosen as well. In this regard, it must be highlighted that a variation of the typical (and extreme) period length implies a change in the model ability to foresee the characteristics of the following days in terms of input, other than a variation in the computational burden. For instance, setting a period length of 7 days has the effect of letting the model know the weather, electricity demand, and electricity market forecasts for a 7 days period.

Typical periods are selected evaluating all the input profiles at once. A weight is hence associated to each typical period, accounting for how many times a particular period is repeated in the newly built aggregated complete period, thus simulating the original one.

Instead, extreme periods have an associated weight equal to 1 (i.e. they are representative of a single period among the total). Also, oppositely to typical periods, extreme ones are selected considering the different profiles individually. These periods are designed so as to enforce the operational feasibility of the system throughout the year, thus improving the k-MILP accuracy by including periods that would be otherwise neglected, even if their impact is limited owing to the little weight associated. In the implemented model, extreme periods can be chosen as the ones in which the peak (min or max) values are present, or as the ones in which the mean over the period correspond to the max or to the min value compared to the one of the other periods.

An example of the clustering results generated by the k-MILP is provided in Figure 4.5. In particular, the figure shows the shapes of the different profiles during the selected 48 h-long typical and extreme periods. Please note that the order here presented is not the one in which they appear in the "synthetic" complete period, they are shown consecutively for visual purposes only. Rather, each of them will be assigned one or multiple times (according to its weight) to different periods of the original complete period.

Finally, the effect of clustering is exemplified in Figure 4.6, which shows the original PV production profile and CSP thermal production profile compared to the "synthetic" ones generated by clustering. The vertical axis shows the hours of the 48 h-long periods, while the horizontal axis shows progressively the period number (as a rescaled time axis). It can be noticed that the original profiles are more indented, indicating a higher level of detail and sensitivity to local/particular phenomena, such as the passing of clouds.

..... ANNUAL???

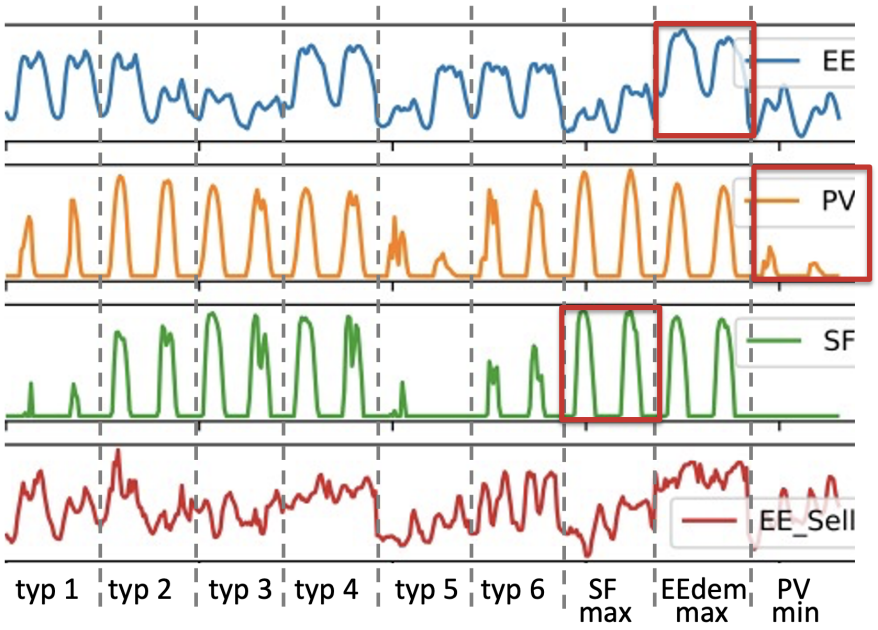

Figure 4.5. An example of typical and extreme periods selected by the k-MILP. From top to bottom: electricity demand; PV production; SF thermal production; power market prices. On the left side 6 typical periods selected, on the rightmost side 3 specified extreme periods

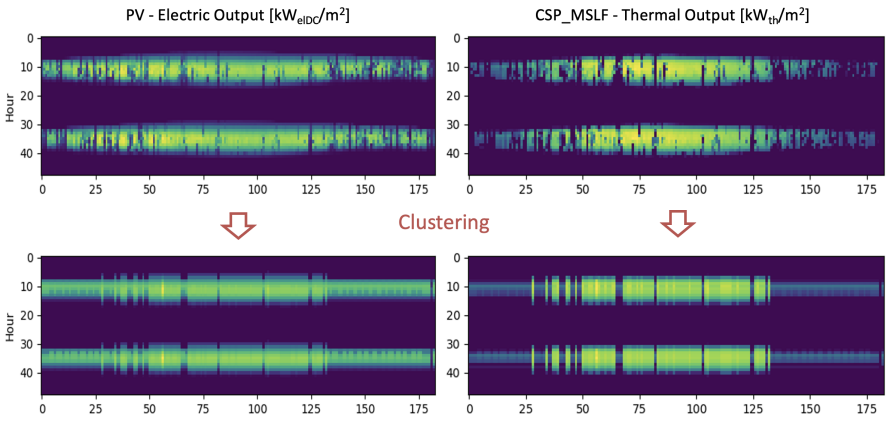

Figure 4.6. Comparison between original (top) and "synthetic" (bottom) profiles

4.3 Endogenous models

Each heat exchanger surface is evaluated by means of the equation 4.11.

$$S_i = \frac{\dot{Q}_i}{U_i \, \Delta T_{ml,i}} \qquad i = HX, HTR, LTR, cooler \tag{4.11}$$

The overall heat transfer coefficients are computed with the equation 4.12.

$$U = \frac{1}{\frac{1}{h_{hot}} + \frac{t_{wall}}{k_{wall}} + \frac{1}{h_{cold}}} \tag{4.12}$$

4.3.1 Sets

In order to... milp spiegazione... the most important sets used in the model are:

- Goods: set including the forms of energy used in the plant:
  - Electrical Energy (EE)
  - Heat
- Demands: subset of energy forms including the ones the plant is required to dispatch:
  - EE
- Machines: set of units producing dispatchable power:
  - PB
- Machines_RES: set of non-dispatchable power-producing systems:
  - PV
  - SF
- Storages: set including energy storage systems:
  - BESS
  - TES

XXXXXXXXXXXXXXXXXX
equations below:

$$\forall \, i \in \, Goods, \forall \, t \tag{4.13}$$

4.3.2 Machines model (equations)

As introduced in Section 4.1.4 ....

$$\eta_{net} = \frac{K_1 \, \dot{Q}_{th,in} + K_2 \, S + K_3}{\dot{Q}_{th,in}} \tag{4.14}$$

In this way the efficiency becomes: (gira equazione yokoyama come in note e citala equation 4.10 (ora è sopra))

4.3.3 Machines_RES model (equations)

(sopra?..simulated exogenously, so the given profiles expressed in kW/m_2 are used by the model...)

$$\sum_i RES_{Area,i} \leq TOT\_ND\_Area \tag{4.15}$$

(..sopra..? model generally no links for the energy flows but every machine can have only certain kinds of inputs and outputs, in some cases, as for the EH, some more specific constraints are needed:

$$ND_{out,i,t} = ND_{profile,i,t}\, ND_{area,i} \tag{4.16}$$

if RES_i is "dissipable" (i.e. its output can be curtailed or somehow diverted):

$$Out_{ND,i,t} \leq ND_{out,i,t} \tag{4.17}$$

else:

$$Out_{ND,i,t} = ND_{out,i,t} \tag{4.18}$$

So:

$$Out_{diss,ND,i,t} = ND_{out,i,t} - Out_{ND,i,t} \tag{4.19}$$

In the case of PV, the output of the array (or part of it) can be diverted to the EH in order to produce heat to be stored in the TES, so the output of the EH is given by the following constraint:

$$EH_{out,t} \leq \sum_i Out_{diss,ND,i,t} \tag{4.20}$$

The efficiency of the EH is currently unitary, but it can be easily modified redefining the variable later.

4.3.4 Storages model (equations)

Moreover, a loss from cold tank has been seen by the model as a negative enthalpy flow has been added to account for PB HX circuit warm-keeping when this unit is turned off

of the units in the Storages set is a measure related to energy, hence its value in time depends also on its status in the previous time instant, as described by the following equation:

$$E_{stor,i,t} = E_{stor,i,t-1}\, \eta_{sd,i} + (Stor_{ch,i,t} - Stor_{disch,i,t})\, dt \tag{4.21}$$

where:

$E_{stor,i,t}$ and $E_{stor,i,t-1}$ are the amounts of energy of the ith storage system at time t and $t-1$ respectively;

$\eta_{sd,i}$ is the self-discharge efficiency of the ith storage system;

$Stor_{ch,i,t}$ and $Stor_{disch,i,t}$ are the charge and discharge powers of the ith storage system at time t;

dt is the model timestep in [h].

An additional term is appended to equation 4.21 in the case of TES in order to account for the additional charge power which can be provided by the EH, thus obtaining equation 4.22:

$$E_{stor,i,t} = E_{stor,i,t}\,\eta_{sd,i} + (Stor_{ch,i,t} - Stor_{disch,i,t})\,dt + EH_{out,t} \tag{4.22}$$

The State Of Charge (SOC) limits (as described in.....) are set by the following equations:

$$E_{stor,max,i} = SOC_{max,i}\,E_{stor,nom,i} \tag{4.23}$$

$$E_{stor,i,t} \leq E_{stor,max,i} \tag{4.24}$$

$$E_{stor,min,i} = SOC_{min,i}\,E_{stor,nom,i} \tag{4.25}$$

$$E_{stor,i,t} \geq E_{stor,min,i} \tag{4.26}$$

The charge and discharge powers of the Storages set units are governed by the following equations:

BESS case: storage power flow is regulated according to limits imposed by C-rate (i.e. ....., see (.....)):

$$Stor_{ch,t} \leq C\text{-}rate_{max}\,E_{stor,nom} \tag{4.27}$$

$$Stor_{disch,t} \leq C\text{-}rate_{max}\,E_{stor,nom} \tag{4.28}$$

TES case: storage maximum charge power is regulated with a power cap logic (... pumps + EH, high value just to impose it physically makes sense...(set equal to C_stor(da fare nel caso) (but never reached?)), while storage maximum discharge power is linked to the PB maximum thermal input:

$$Stor_{ch,t} \leq P_{in,max,TES} \tag{4.29}$$

$$P_{out,max,TES} = \dot{Q}_{th,in,PB}/\eta_{disch,TES} \tag{4.30}$$

$$Stor_{disch,t} \leq P_{out,max,TES} \tag{4.31}$$

XXXXXXX

4.3.5 model energy bal(equations)

$$Mach_{out,i,t} + Out_{ND,i,t} + Stor_{exch,i,t} - Mach_{IntCons,i,t} + Slack_{i,t} = Demand_{i,t} \quad (4.32)$$

where:

$Mach_{out,i,t}$ is the output of the units of the Machines set, so in this case the EE output of the PB only;

$Out_{ND,i,t}$ is described in equation 4.17

$Stor_{exch,i,t}$ is the net energy output of the units of the Storage set, defined as:

$$Stor_{exch,i,t} = Stor_{disch,i,t}\, \eta_{disch,i} - Stor_{ch,i,t}/\eta_{ch,i} \quad (4.33)$$

$Mach_{IntCons,i,t}$ is the input of a subset of the Machines set, Machines_IntCons, which includes only the machines which use an internally produced good as an input. In this model it hence refers to the PB heat input only;

$Slack_{i,t}$ is the penalty attributed to the non-produced energy as described in..... ;

$Demand_{i,t}$ is the Demand profile as described in ..... .

4.4 Optimisation options

schemone + eventuali equazioni/schemi legati a queste particolari operation/opzioni

4.5 economic inputs

PV: formula con size*eta (da PVwatts help) per passare a /m2
Solar tower piecewise...

4.6 Model test with reference existing plant

Cerro Dominador paramters + weather files, ... LCOE, CF, clustering, PPA..

*inverter: DC to AC ratio (not in the model, assumed to 1.2 as typical and does not limit, checked from simulation, + typical since typical total installed costs are used). +spento sotto 10% da documento tecnico PV partanna. + efficienza presa da SAM e comunque valore tipico: 97%. Assunta costante because of MILP limits (non-linearities would otherwise arise), reasonable because actually it is more or less except at very low loads.

*scrivere da qualche parte che impianto non può importare elettricità dalla rete, salvo modifiche...

Chapter 5

Results and discussion

Conclusions

Lorem ipsum dolor sit amet, consectetur adipisci elit, sed eiusmod tempor incidunt ut labore et dolore magna aliqua. Ut enim ad minim veniam, quis nostrum exercitationem ullam corporis suscipit laboriosam, nisi ut aliquid ex ea commodi consequatur.

Appendix A

First Appendix

Lorem ipsum dolor sit amet, consectetur adipisci elit, sed eiusmod tempor incidunt ut labore et dolore magna aliqua. Ut enim ad minim veniam, quis nostrum exercitationem ullam corporis suscipit laboriosam, nisi ut aliquid ex ea commodi consequatur.

Acronyms

BESS	Battery Energy Storage System
BEV	Battery Electric Vehicle
CF	Capacity Factor
COP21	2015 United Nations Climate Change Conference, also known as the Paris Climate Conference
CPV	Concentrated Photovoltaic
CR	Concentration Ratio
CSP	Concentrated Solar Power
DNI	Direct Normal Irradiance
DoD	Depth of Discharge
DSG	Direct Steam Generation
EDNI	Effective Direct Normal Irradiance
EH	Electric Heater
EE	Electrical Energy
EMS	Energy Management System
GCR	Ground Coverage Ratio
GHG	Greenhouse Gas
HJT	Hetero Junction Technology
HTF	Heat Transfer Fluid
HTHP	High Temperature Heat Pump
HX	Heat Exchanger
LCOE	Levelised Cost Of Electricity
LDC	Load Duration Curve
LF	Linear Fresnel
MILP	Mixed Integer Linear Programming
MINLP	Mixed Integer Nonlinear Programming
MPPT	Maximum Power Point Tracking
MSLF	Molten Salts Linear Fresnel
MSPT	Molten Salts Parabolic Trough

MV	Medium Voltage
NOCT	Nominal Operating Cell Temperature
ORC	Organic Rankine Cycle
PB	Power Block
PCM	Phase Change Material
PPA	Power Purchase Agreement
PT	Parabolic Trough
PUN	Prezzo Unico Nazionale
PV	Photovoltaic
P2TESc	Power to cold tank
P2TESh	Power to hot tank
RES	Renewable Energy Sources
RH	Relative Humidity
SBS	Spectral Beam Splitting
sCO$_2$	Supercritical CO_2
SF	Solar Field
SFrec	Solar Field recirculation
SFwk	Solar Field warm-keeping
SM	Solar Multiple
SOC	State Of Charge
SRC	Steam Rankine Cycle
STC	Standard Test Conditions
TES	Thermal Energy Storage
TIT	Turbine Inlet Temperature
TMY	Typical Meteorological Year
VRFB	Vanadium Redox Flow Battery

Bibliography

[1] NOAA Climate.gov, "CO_2 in the atmosphere and annual emissions (1750-2019)," https://www.climate.gov/news-features/understanding-climate/climate-change-atmospheric-carbon-dioxide, 2020, accessed: 2020-11-29.

[2] Our World in Data, "Sector by sector: where do global greenhouse gas emissions come from?" https://ourworldindata.org/ghg-emissions-by-sector, 2020, accessed: 2020-11-30.

[3] IEA, "Global CO_2 emissions in 2019," https://www.iea.org/articles/global-co2-emissions-in-2019, 2020, accessed: 2020-12-01.

[4] IEA, "World energy outlook 2020," https://www.iea.org/reports/world-energy-outlook-2020, 2020, accessed: 2020-12-01.

[5] "European union 2020," IEA, Paris, FR, Tech. Rep., Jun. 2020.

[6] I. M. of Economic Development, "Italy's national energy strategy 2017," 2017.

[7] World Energy Council, "\"energy trilemma\"," https://www.worldenergy.org/transition-toolkit/world-energy-trilemma-index, 2020, accessed: 2020-12-08.

[8] M. Kamran, M. R. Fazal, M. Mudassar, S. R. Ahmed, M. Adnan, I. Abid, F. J. S. Randhawa, and H. Shams, "Solar photovoltaic grid parity: A review of issues and challenges and status of different pv markets," *International Journal of Renewable Energy Research*, vol. 9, 2019.

[9] V. Shah, J. Booream-Phelps, and S. Min, "2014 outlook: Let the second gold rush begin," Deutsche Bank Market Research, Tech. Rep., Jan. 2014. [Online]. Available: https://www.deutschebank.nl/nl/docs/Solar_-_2014_Outlook_Let_the_Second_Gold_Rush_Begin.pdf

[10] P. Denholm, E. Ela, B. Kirby, and M. Milligan, "Role of energy storage with renewable electricity generation," Jan. 2010.

[11] P. Ruiz, W. Nijs, D. Tarvydas, A. Sgobbi, A. Zucker, R. Pilli, R. Jonsson, A. Camia, C. Thiel, C. Hoyer-Klick, F. Dalla Longa, T. Kober, J. Badger, P. Volker, B. Elbersen, A. Brosowski, and D. Thrän, "Enspreso - an open, eu-28 wide, transparent and coherent database of wind, solar and biomass energy potentials," *Energy Strategy Reviews*, vol. 26, p. 100379, 2019.

[12] IRENA, "Renewable power generation costs in 2019," International Renewable Energy Agency, Abu Dhabi, Tech. Rep., 2020.

[13] A. R. Starke, J. M. Cardemil, R. Escobar, and S. Colle, "Multi-objective optimization of hybrid CSP+PV system using genetic algorithm," *Energy*, vol. 147, pp. 490–503, Mar. 2018.

[14] L. Bousselamti and M. Cherkaoui, "Modelling and assessing the performance of hybrid pv-csp plants in morocco: A parametric study," *International Journal of Photoenergy*, vol. 2019, 2019.

[15] C. S. Lai and M. D. McCulloch, "Levelized cost of electricity for solar photovoltaic and electrical energy storage," *Applied Energy*, vol. 190, pp. 191–203, 2017.

[16] R. Małkowski, M. Jaskólski, and W. Pawlicki, "Operation of the hybrid photovoltaic-battery system on the electricity market-simulation, real-time tests and cost analysis," *Energies*, vol. 16, Mar. 2020.

[17] Y. Shibata, "How can "solar pv + battery system" be economically competitive and reliable power generation? - Strategies for post-fit."

[18] D. Feldman, R. Margolis, P. Denholm, and J. Stekli, "Exploring the potential competitiveness of utility-scale photovoltaics plus batteries with concentrating solar power, 2015-2030," 2016.

[19] SEA, "Ficha del proyecto: Planta solar cerro dominador," https://seia.sea.gob.cl/expediente/ficha/fichaPrincipal.php?modo=ficha&id_expediente=2128879352, 2014, accessed: 2020-12-15.

[20] M. Petrollese, G. Cau, and D. Cocco, "The ottana solar facility: dispatchable power from small-scale CSP plants based on ORC systems," *Renewable Energy*, vol. 147, pp. 2932–2943, Mar. 2020.

[21] S. Kraemer, "Morocco pioneers PV with thermal storage at 800 mw midelt csp project," https://www.solarpaces.org/morocco-pioneers-pv-to-thermal-storage-at-800-mw-midelt-csp-project, 2020, accessed: 2021-01-20.

[22] SNAM and McKinsey, "The hydrogen challenge: The potential of hydrogen in italy," SNAM, Milan, Italy, Tech. Rep., 2019.

[23] S. Jewkes, "Italy can be clean energy hub with hydrogen imports from africa, study says," https://www.reuters.com/article/us-italy-hydrogen-idUSKBN25W0JM, Sep. 2020, accessed: 2021-03-07.

[24] T. Crescenzi, M. Falchetta, A. Fontanella, E. Metelli, A. Miliozzi, F. Spinelli, and L. Sipione, *Opportunità di applicazione delle tecnologie solari termodinamiche in Italia*. ENEA, 2016.

[25] CSP Focus, "Promising test results for molten salts in trough csp," http://www.cspfocus.cn/en/market/detail_3258.htm, 2020, accessed: 2021-02-15.

[26] M. Günther, M. Eickhoff, T. Khalil, and M. Meyer-Grünefeldt, *Advanced CSP Teaching Materials - Chapter 6: Linear Fresnel Technology*, 2011, p. 34.

[27] J. Coventry, C. Andraka, J. Pye, M. Blanco, and J. Fisher, "A review of sodium receiver technologies for central receiver solar power plants," *Solar Energy*, vol. 122, pp. 749–762, 2015.

[28] 1414 Degrees, "What is 1414 degrees?" https://1414degrees.com.au/what, 2020, accessed: 2021-02-16.

[29] O. Achkari and A. El Fadar, "Latest developments on tes and csp technologies – energy and environmental issues, applications and research trends," *Applied Thermal Engineering*, vol. 167, p. 114806, 2020.

[30] S. R. Pendem and S. Mikkili, "Modeling, simulation and performance analysis of solar PV array configurations (series, series–parallel and honey-comb) to extract maximum power under partial shading conditions," *Energy Reports*, vol. 4, pp. 274–287, 2018.

[31] "A quantitative comparison of central inverters and string inverters in utility-scale solar systems in north america," http://solar.schneider-electric.com/wp-content/uploads/2016/11/20161201-A-Quantitative-Comparison-of-Central-Inverters-and\-String-Inverters-in-Utility-Scale-Solar-Systems-in-North-America-.pdf, Schneider Electric, Tech. Rep., 2016, accessed: 2021-02-22.

[32] K. Misbrener, "How to choose between string and central inverters in utility-scale installations," https://www.solarpowerworldonline.com/2018/12/choose-between-string-and-central-inverters-utility-scale-solar, Dec. 2020, accessed: 2021-02-22.

[33] F. Colville, "Monocrystalline cells dominate solar photovoltaic industry, but technology roadmap is far from certain," https://www.laserfocusworld.com/photonics-business/article/14184986/monocrystalline-cells-dominate-solar-photovoltaic-industry-but-\technology-roadmap-is-far-from-certain, Nov. 2020, accessed: 2021-02-22.

[34] P. Roy, N. Kumar Sinha, S. Tiwari, and A. Khare, "A review on perovskite solar cells: Evolution of architecture, fabrication techniques, commercialization issues and status," *Solar Energy*, vol. 198, pp. 665–688, 2020.

[35] A. Green, C. Diep, R. Dunn, and J. Dent, "High capacity factor CSP-PV hybrid systems," vol. 69. Elsevier Ltd, May 2015, pp. 2049–2059.

[36] C. Kost, J. N. Mayer, J. Thomsen, N. Hartmann, C. Senkpiel, S. P. Philipps, S. Nold, S. Lude, N. Saad, J. Schmid, and T. Schlegl, "Levelized cost of

electricity: PV and CPV in comparison to other technologies," Fraunhofer Institute for Solar Energy Systems ISE, Tech. Rep., 2014.

[37] C. D. Rodríguez-Gallegos, H. Liu, O. Gandhi, J. P. Singh, V. Krishnamurthy, A. Kumar, J. S. Stein, S. Wang, L. Li, T. Reindl, and I. M. Peters, "Global techno-economic performance of bifacial and tracking photovoltaic systems," *Joule*, vol. 4, no. 7, pp. 1514–1541, 2020.

[38] EIA, S. Hoff, and J. DeVilbiss, "More than half of utility-scale solar photovoltaic systems track the sun through the day," https://www.eia.gov/todayinenergy/detail.php?id=30912#, Apr. 2017, accessed: 2021-02-23.

[39] IRENA, "Electricity storage and renewables: Costs and markets to 2030," International Renewable Energy Agency, Abu Dhabi, Tech. Rep., 2017.

[40] ——, "Innovation landscape brief: Utility-scale batteries," International Renewable Energy Agency, Abu Dhabi, Tech. Rep., 2019.

[41] M. Moser, F. Trieb, T. Fichter, and J. Kern, "Integrated techno-economic assessment of hybrid CSP-PV plants," vol. 2033. American Institute of Physics Inc., Nov. 2018.

[42] A. Zurita, C. Mata-Torres, J. M. Cardemil, and R. A. Escobar, "Assessment of time resolution impact on the modeling of a hybrid CSP-PV plant: A case of study in chile," *Solar Energy*, vol. 202, pp. 553–570, May 2020.

[43] W. Hamilton, M. Husted, A. Newman, R. Braun, and M. Wagner, "Dispatch optimization of concentrating solar power with utility-scale photovoltaics," *Optimization and Engineering*, 2019.

[44] A. Zurita, C. Mata-Torres, C. Valenzuela, C. Felbol, J. M. Cardemil, A. M. Guzmán, and R. A. Escobar, "Techno-economic evaluation of a hybrid CSP+PV plant integrated with thermal energy storage and a large-scale battery energy storage system for base generation," *Solar Energy*, vol. 173, pp. 1262–1277, Oct. 2018.

[45] L. Migliari, "Modelling and analysis of medium-size hybrid CSP-CPV systems designed for improving the dispatchability of solar power plants," Ph.D. dissertation, Università degli Studi di Cagliari, 2017.

[46] G. Cau, D. Cocco, and M. Petrollese, "Optimal energy management strategy for CSP-CPV integrated power plants with energy storage," in *Proceedings of Ecos 2015 - The 28th International Conference on Efficiency, Cost, Optimization, Simulation and Environmental Impact of Energy Systems*, Pau, France, 2015.

[47] R. Zhai, Y. Chen, H. Liu, H. Wu, Y. Yang, and M. O. Hamdan, "Optimal design method of a hybrid CSP-PV plant based on genetic algorithm considering the operation strategy," *International Journal of Photoenergy*, vol. 2018, 2018.

[48] D. Cocco, L. Migliari, and M. Petrollese, "A hybrid CSP-CPV system for improving the dispatchability of solar power plants," *Energy Conversion and Management*, vol. 114, pp. 312–323, Apr. 2016.

[49] M. Falchetta, D. Mazzei, V. Russo, V. A. Campanella, V. Floridia, B. Schiavo, L. Venezia, C. Brunatto, and R. Orlando, "The Partanna project: A first of a kind plant based on molten salts in LFR collectors," *AIP Conference Proceedings*, vol. 2303, no. 1, p. 040001, 2020.

[50] K.-J. Riffelmann, G. Weinrebe, and M. Balz, "Hybrid CSP-PV plants with integrated thermal storage," in *Proceedings of the 26th SolarPaces Conference*, 2020.

[51] Y. Gedle, M. Schmitz, H. Gielen, P. Schmitz, U. Herrmann, C. T. Boura, Z. Mahdi, R. Alexander, C. Caminos, and J. Dersch, "Analysis of an integrated CSP-PV hybrid power plant," in *Proceedings of the 26th SolarPaces Conference*, 2020.

[52] Z. Mahdi, J. Dersch, P. Schmitz, S. Dieckmann, R. Alexander, C. Caminos, C. T. Boura, U. Herrmann, C. Schwager, M. Schmitz, H. Gielen, Y. Gedle, and R. Büscher, "Technical assessment of brayton cycle heat pumps for the integration in hybrid PV-CSP power plants," in *Proceedings of the 26th SolarPaces Conference*, 2020.

[53] R. B. Laughlin, "Pumped thermal grid storage with heat exchange," *Journal of Renewable and Sustainable Energy*, vol. 9, no. 4, p. 044103, 2017.

[54] X. Ju, C. Xu, Y. Hu, X. Han, G. Wei, and X. Du, "A review on the development of photovoltaic/concentrated solar power (PV-CSP) hybrid systems," *Solar Energy Materials and Solar Cells*, vol. 161, pp. 305–327, Mar. 2017.

[55] T. P. Otanicar, S. Theisen, T. Norman, H. Tyagi, and R. A. Taylor, "Envisioning advanced solar electricity generation: Parametric studies of CPV/T systems with spectral filtering and high temperature PV," *Applied Energy*, vol. 140, pp. 224–233, 2015.

[56] I. E. Grossmann, "Advances in mathematical programming models for enterprise-wide optimization," *Computers & Chemical Engineering*, vol. 47, pp. 2–18, 2012.

[57] L. Urbanucci, "Limits and potentials of mixed integer linear programming methods for optimization of polygeneration energy systems," *Energy Procedia*, vol. 148, pp. 1199–1205, 2018, aTI 2018 - 73rd Conference of the Italian Thermal Machines Engineering Association.

[58] R. Lamedica, E. Santini, A. Ruvio, L. Palagi, and I. Rossetta, "A milp methodology to optimize sizing of pv - wind renewable energy systems," *Energy*, vol. 165, pp. 385–398, Dec. 2018.

[59] M. Petrollese, D. Cocco, G. Cau, and E. Cogliani, "Comparison of three different approaches for the optimization of the csp plant scheduling," *Solar Energy*, vol. 150, pp. 463–476, Jul. 2017.

[60] K. M. Powell, J. D. Hedengren, and T. F. Edgar, "Dynamic optimization of a hybrid solar thermal and fossil fuel system," *Solar Energy*, vol. 108, pp. 210–218, 2014.

[61] M. Nemati, M. Braun, and S. Tenbohlen, "Optimization of unit commitment and economic dispatch in microgrids based on genetic algorithm and mixed integer linear programming," *Applied Energy*, vol. 210, pp. 944–963, 2018.

[62] S. Mazzola, C. Vergara, M. Astolfi, V. Li, I. Perez-Arriaga, and E. Macchi, "Assessing the value of forecast-based dispatch in the operation of off-grid rural microgrids," *Renewable Energy*, vol. 108, pp. 116–125, 2017.

[63] J. R. Birge and F. Louveaux, *Introduction to Stochastic Programming*, 2nd ed. Springer Publishing Company, Incorporated, 2011.

[64] A. Ben-Tal, L. E. Ghaoui, and A. Nemirovski, *Robust optimization*. Princeton University Press, 2009, vol. 28.

[65] R. Dominguez, L. Baringo, and A. J. Conejo, "Optimal offering strategy for a concentrating solar power plant," *Applied Energy*, vol. 98, pp. 316–325, Oct. 2012.

[66] J. Usaola, "Operation of concentrating solar power plants with storage in spot electricity markets," *IET Renewable Power Generation*, vol. 6, pp. 59–66, Jan. 2012.

[67] C. A. Pan, R. Guédez, F. Dinter, and T. M. Harms, "A techno-economic comparative analysis of thermal oil and molten salt parabolic trough power plants with molten salt solar towers," vol. 2126. American Institute of Physics Inc., Jul. 2019.

[68] M. Falchetta, D. Mazzei, V. Russo, V. A. Campanella, V. Floridia, B. Schiavo, L. Venezia, C. Brunatto, and R. Orlando, "The partanna project: A first of a kind plant based on molten salts in lfr collectors," *AIP Conference Proceedings*, vol. 2303, no. 1, p. 040001, 2020.

[69] "Il solare termodinamico a concentrazione - la nuova frontiera dei sali fusi," http://www.archimedesolarenergy.it/brochure_ase.pdf, Archimede Solar Energy srl, 2016, accessed: 2021-03-11.

[70] "Solar power on demand - least cost opportunity for sun-rich countries," https://www.frenell.de/wp-content/uploads/2016/05/FRENELL_White_Paper_V1.0_May_2016.pdf, FRENELL GmbH, 2016, accessed: 2021-03-17.

[71] Sol.In.Par. and C.&C. Consulting Engineering S.r.l., "Relazione tecnica specialistica impianto csp," https://si-vvi.regione.sicilia.it/viavas/index.php/it/component/fabrik/list/28/it/?Itemid=&integrazioni___id_integrazioni_raw=304&limitstart28=0&resetfilters=1, 2020, accessed: 2021-03-17.

[72] A. Giaconia, R. Grena, and V. Russo, "Definizione delle configurazioni di impianti ibridi CSP/PV più idonee all'interfacciamento con il sistema di distribuzione di energia elettrica nazionale," ENEA, Rome, Italy, Tech. Rep., 2019.

[73] C. Thompson, "AC vs. DC coupling in utility-scale solar plus storage projects," Eaton, Cleveland, OH, United States, Tech. Rep., 2016.

[74] J. He, Y. Yang, and D. Vinnikov, "Energy storage for 1500 V photovoltaic systems: A comparative reliability analysis of DC- and AC-coupling," *Energies*, vol. 13, no. 13, 2020.

[75] "Explorador Solar," http://ernc.dgf.uchile.cl:48080/exploracion, Ministerio de Energia Gobierno de Chile, 2021, accessed: 2021-01-25.

[76] R. Chico Caminos, "Techno-economic assessment of hybrid photovoltaic/solar thermal power plants: Modeling and potential for synergies," Nov. 2017.

[77] Abengoa Solar, "Proyecto planta solar cerro dominador atacama 1 - presentación cuenta regresiva hacia la cop21 desafíos actuales," Oct. 2015.

[78] Gestore Servizi Energetici, "Incentivazione della produzione di energia elettrica da impianti a fonti rinnovabili diversi dai fotovoltaici," Jul. 2016.

[79] M. Petrollese and D. Cocco, "Optimal design of a hybrid CSP-PV plant for achieving the full dispatchability of solar energy power plants," *Solar Energy*, vol. 137, pp. 477–489, 11 2016.

[80] J. Hernández-Moro and J. Martínez-Duart, "Analytical model for solar pv and csp electricity costs: Present lcoe values and their future evolution," *Renewable and Sustainable Energy Reviews*, vol. 20, pp. 119–132, 2013.

[81] National Renewable Energy Laboratory, "System Advisor Model," https://sam.nrel.gov, Golden, CO, USA, accessed: 2020-11-10.

[82] *SAM's Help system*, National Renewable Energy Laboratory, Golden, CO, USA, 2020, p. 636.

[83] ENEA, "Personal communication," 2020.

[84] M. Zatti, "Optimal design of urban energy districts under uncertainty," Ph.D. dissertation, Politecnico di Milano, 2019.

[85] M. Zatti, M. Gabba, M. Freschini, M. Rossi, A. Gambarotta, M. Morini, and E. Martelli, "k-milp: A novel clustering approach to select typical and extreme days for multi-energy systems design optimization," *Energy*, vol. 181, pp. 1051–1063, 2019.